ACS OMEGA

Open Access

http://pubs.acs.org/journal/acsodf

Review

Progress in Research on Inhibitors Targeting SARS-CoV-2 Main Protease (M^{pro})

Yue Yang,[#] Yi-Dan Luo,[#] Chen-Bo Zhang,[#] Yang Xiang,[#] Xin-Yue Bai, Die Zhang, Zhao-Ying Fu, Ruo-Bing Hao, and Xiao-Long Liu*

Cite This: *ACS Omega* 2024, 9, 34196−34219

Read Online

ACCESS | Metrics & More | Article Recommendations

ABSTRACT: Since 2019, the novel coronavirus (SARS-CoV-2) has caused significant morbidity and millions of deaths worldwide. The Coronavirus Disease 2019 (COVID-19), caused by SARS-CoV-2 and its variants, has further highlighted the urgent need for the development of effective therapeutic agents. Currently, the highly conserved and broad-spectrum nature of main proteases (M^{pro}) renders them of great importance in the field of inhibitor study. In this study, we categorize inhibitors targeting M^{pro} into three major groups: mimetic, nonmimetic, and natural inhibitors. We then present the research progress of these inhibitors in detail, including their mechanism of action, antiviral activity, pharmacokinetic properties, animal experiments, and clinical studies. This review aims to provide valuable insights and potential avenues for the development of more effective antiviral drugs against SARS-CoV-2.

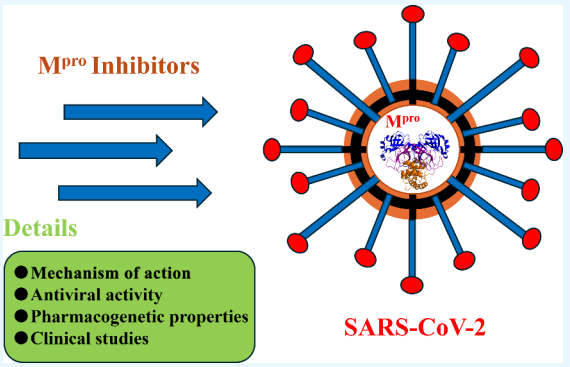

1. INTRODUCTION

The Coronavirus Disease 2019 (COVID-19) has significantly impacted the global economy and public health systems.[1,2] COVID-19, caused by the highly infectious and mutable Severe Acute Respiratory Syndrome Coronavirus 2 (SARS-CoV-2), has seen its Omicron variant supplant the Delta variant, subsequently mutating into various new strains. This evolution presents substantial challenges to healthcare systems and the public health infrastructure.[3−7] Despite the transition of the COVID-19 outbreak toward a more normalized phase, ongoing research into inhibitors remains crucial for the preemptive prevention of future coronavirus pandemics.[8,9]

COVID-19, a respiratory ailment, is propagated by SARS-CoV-2, a positive-sense single-stranded RNA virus.[10] This virus is composed of structural proteins, including the nucleocapsid protein (N), spike protein (S), envelope protein (E), and membrane glycoprotein (M), along with an RNA genome. It, along with SARS-CoV, HCoV-OC43, HCoV-HKU1, and MERS-CoV, is part of the β-coronavirus genus.[11] The replication process of SARS-CoV-2 involves several critical steps: initially, the virus' S protein binds to the angiotensin-converting enzyme 2 (ACE2) receptor on host cells or enters directly via cytosis, releasing the viral RNA. Subsequently, the host's transmembrane serine protease 2 (TMPRSS2) cleaves and merges with the viral S protein, facilitating entry and RNA release into the host cell. Viral replication and assembly then occur with the assistance of nonstructural proteases, such as the papain-like protease PL^{pro} (nsp3), the main protease M^{pro} (nsp5), and the RNA-dependent RNA polymerase RdRp (nsp12).[12−14] Finally, newly formed viruses are released from the cell to infect others, perpetuating the viral life cycle[15,16] (Figure 1).

The above suggests that both viral (structural and nonstructural) and host (ACE2 and TMPRSS2) proteins are pivotal in the viral replication cycle. Targeting these proteins provides a strategic approach to inhibiting viral replication.[17,18] Structural proteins, particularly S proteins, are instrumental in viral pathogenesis through receptor recognition and membrane fusion. E proteins, despite being the smallest structural proteins, play a crucial role in viral assembly, budding, envelope formation, and pathogenicity. M proteins are key in viral assembly, whereas N proteins serve multiple functions, including packaging the viral RNA genome. In host proteins, ACE2 acts as the primary gateway for the virus to enter cells, making it a focal point for blocking viral entry. TMPRSS2, prevalent in human gastrointestinal, genitourinary, and respiratory epithelia, is essential for activating coronavirus S proteins, thus facilitating SARS-CoV-2 infection. These insights reveal that each protein plays a significant role in

Received: April 1, 2024
Revised: July 12, 2024
Accepted: July 19, 2024
Published: August 2, 2024

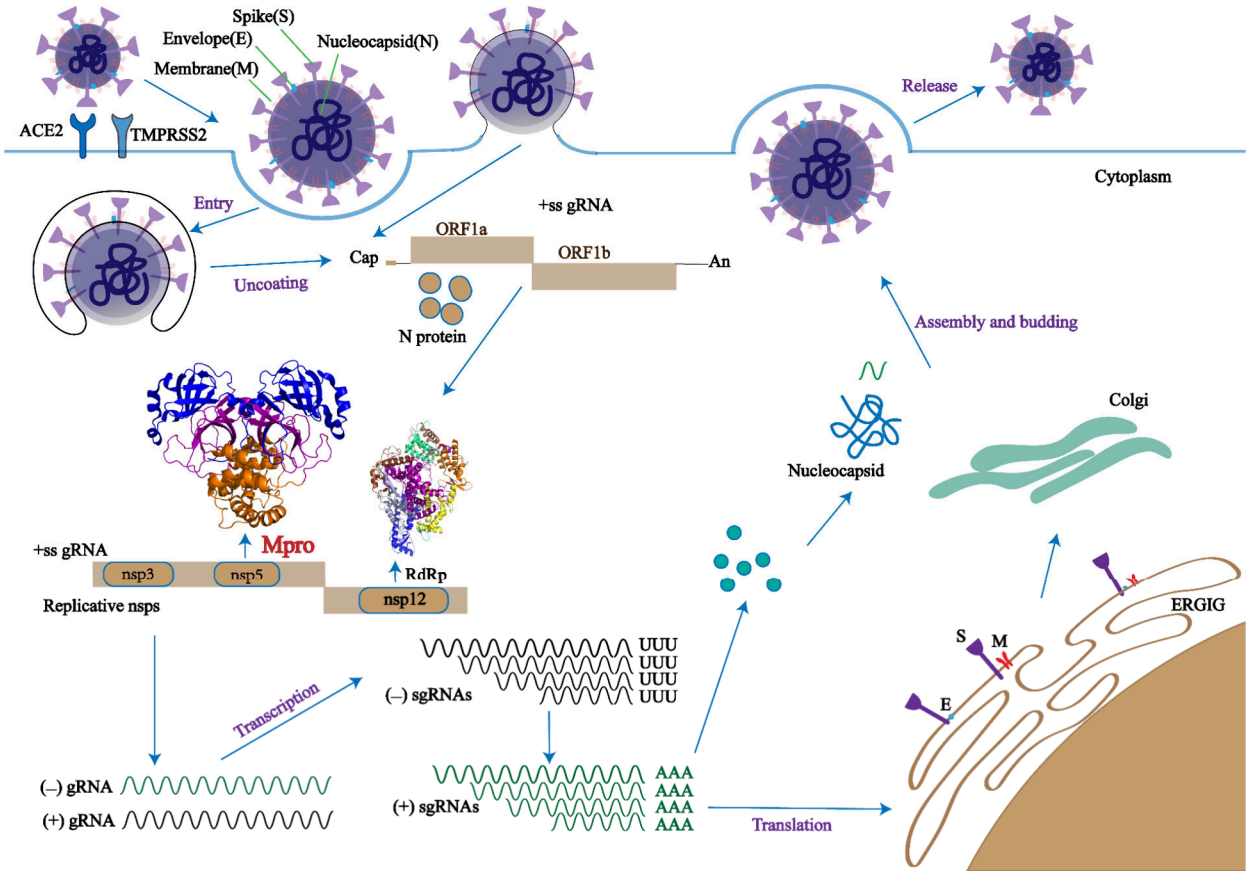

Figure 1. Coronavirus particles are composed of four structural proteins, namely, S protein, E protein, M protein, and N protein. S, M, and E are doped into the viral particle when the RNA genome is wrapped in N. Coronavirus particles bind to cell attachment factors, facilitating their uptake and fusion in cell membranes or endosomal membranes. Upon entry, the RNA genome is released, decapsulated, and immediately translated by ORF1a and ORF1b. The resulting polyproteins, pp1a and pp1ab, undergo cotranslation and post-translational processing into individual nonstructural proteins (nsps) that form the viral replication and transcription complex (RTC). Then RTC replicates the viral genome to the negatively stranded genomic RNA. Translated E and M facilitate virus assembly and budding by interacting with other viral proteins. Viruses budding into the ERGIC lumen reach the plasma membrane by secretion, and virus-containing vesicles are released outside the cell after fusion with the plasma membrane.

viral proliferation. However, challenges arise due to the virus' propensity for mutation (e.g., S proteins) and the varied expression of receptor proteins (e.g., ACE2) across different tissues, complicating the development of effective inhibitors. Interestingly, the nonstructural proteins of SARS-CoV-2, such as M^{pro} and RdRp, are highly conserved across virus strains, making them attractive targets for drug development that minimize interference with host cell physiological processes.[19−21] Notably, M^{pro}'s unique substrate specificity—cleaving peptides only after glutamine residues, a feature not shared by any human protease—reduces the potential for host cell toxicity from M^{pro}-targeting inhibitors. Leveraging drug repurposing and design strategies, researchers have identified numerous inhibitors targeting SARS-CoV-2 M^{pro}. Consequently, this paper focuses on investigating anti-SARS-CoV-2 drugs targeting M^{pro}, highlighting its importance as a target for therapeutic development.

2. STRUCTURE AND FUNCTION OF SARS-COV-2 M^{PRO}

The main protease (M^{pro}) of SARS-CoV-2, a 33 kDa cysteine protease, also known as Nsp5 or 3C-like protease ($3CL^{pro}$), is a crucial target for COVID-19 drug development.[22] It shares a remarkable 96% sequence similarity with SARS-CoV M^{pro}, underscoring the potential for broad-spectrum antiviral inhibitors.[23] M^{pro} facilitates the cleavage of the pp1a and pp1ab polyproteins at 11 distinct sites, yielding 12 functional proteins essential for viral replication. Given its highly conserved nature and specific function, M^{pro} stands out as a prime candidate for therapeutic intervention against the bacterium's COVID-19. Inhibitors designed to target M^{pro} could effectively halt the virus' life cycle, offering a strategy to combat the infection.

M^{pro}'s structure is divided into three domains: I, II, and III. The active site of the protease is located at the junction of domains I and II, where it is split into four subsites: S1, S1′, S2, and S4. These subsites interact with specific fragments of inhibitors (P1, P1′, P2, and P3) with a high binding affinity, a crucial factor for inhibitory effectiveness (Figure 2). The S1′ pocket contains the nucleophilic −SH of Cys145, which can be deprotonated by His41 to create activated thiolate ions, forming a stable "oxyanion cave" for electrophilic reagent binding. The S1 pocket, specific for glutamine, includes Phe140, His163, His164, Glu166, and His172. The hydrophobic S2 (Met49, Tyr54, Met165, Pro168, Val186) and S4 (Gln189, Ala191, Gln192, Gly251) pockets interact with corresponding functional groups.[24] M^{pro}-type inhibitors require small hydrophobic residues at the P1 subsite and Gln residues at the P1′ subsite. Additionally, large hydrophobic residues,

https://doi.org/10.1021/acsomega.4c03023
ACS Omega 2024, 9, 34196−34219

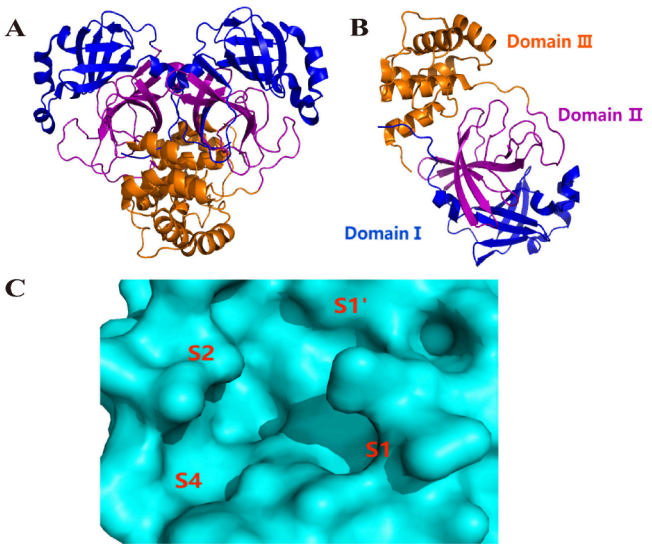

Figure 2. Crystal structure of M^{pro} (A) (PBD ID: 7BB2). The structural region of M^{pro} (B) (PBD ID: 7ALH). The cavity structure of M^{pro} (C).

like aromatic rings for $\pi-\pi$ stacking interactions, are preferred at the P2 site.[25,26] Studies show that forming a covalent bond between an inhibitor's P1′ segment and the Cys-145 residue in the S1′ subsite significantly boosts the inhibitor's antiviral activity.[27,28]

One of the key advantages of targeting M^{pro} is its highly conserved substrate recognition site, which differs from that of known human proteases. This unique feature results in exceptional selectivity and safety for M^{pro} inhibitors, reducing the likelihood of unintended side effects. Therapeutic options for M^{pro} include both existing drugs like Paxlovid and those currently being studied in clinical trials[17,29] (Table 1). This review will delve into the realm of M^{pro} inhibitors, covering synthetic and naturally occurring compounds and shedding light on their potential in combating COVID-19.

3. INHIBITORS TARGETING M^{PRO}

3.1. Peptidomimetic Inhibitors. Peptidomimetic inhibitors, a class of inhibitors that mimic the natural structure of peptides or proteins, have shown promise in drug development.[55] Specifically, covalent peptidomimetic inhibitors have emerged as the most advanced, with a key feature being their similarity to the natural peptide substrate of the M^{pro}. These inhibitors interact with biological targets like the original substrate. Many of these inhibitors contain electrophilic "warhead" groups designed to covalently bind with the nucleophilic SH group of Cys145, which is a common strategy in the development of anti-COVID-19 drugs.[56]

3.1.1. Ketone-Containing Inhibitors. Chen's team[42] developed a potent M^{pro} inhibitor, **RAY1216**, featuring an α-ketoamide warhead, aiming to improve inhibitor efficacy (Figure 3A). Kinetic enzyme inhibition analysis revealed that **RAY1216** employs a slow-tight binding mechanism (K_i = 8.6 nM), significantly enhancing its inhibitory effect. Tested in VeroE6 cells, **RAY1216** exhibited minimal toxicity (CC_{50} = 511 μM) and demonstrated robust inhibitory activity across various SARS-CoV-2 strains, including the original strain (EC_{50} = 95 nM), Delta (EC_{50} = 97 nM), and Omicron subvariants BA.1 (EC_{50} = 86 nM) and BA.5 (EC_{50} = 158 nM), indicating its broad-spectrum potential against SARS-CoV-2. In an ACE2 transgenic mouse model, **RAY1216** markedly reduced the viral load in lung tissue. Notably, its elimination half-life ranged from 2.6 to 14.9 h across different animal models, offering an improved pharmacokinetic profile compared to PF-07321332. The crystallographic data show **RAY1216** covalently bonds to M^{pro}, forming a sulfur thiohemiketal bond with Cys145 and facilitating an "oxygen anion hole" through interactions at the P1′ site, enhancing its antiviral mechanism (Figure 3E). As of March 21, 2023, **RAY1216** has been authorized as a COVID-19 therapeutic,

Table 1. Marketed and Clinical-Stage Drugs Targeting M^{pro}

Drug name	First R&D company	Highest R&D stage worldwide	Listed countries
nirmatrelvir + ritonavir[29−35]	Pfizer	Approval for listing	USA, Korea, UK, Iceland, Liechtenstein, Norway, EU, Japan, Israel, China
SIM-0417[36−38]	Shanghai Institute of Pharmaceutical Sciences, Chinese Academy of Sciences	Approval for listing	China
ensitrelvir[39−41]	Shionogi, Inc.	Approval for listing	Japan
RAY-1216[42]	Guangdong Zhongsheng Pharmaceutical Co., Ltd.	Approval for listing	China
GST-HG171[43−45]	Fujian Guangshengtang Pharmaceutical Co., Ltd.	Approval for listing	China
WPV-01[46,47]	Westlake University	Phase III Clinical	
FB-2001[48]	Shanghai Institute of Materia Medica, Chinese Academy of Sciences	Phase III Clinical	
Carrimycin[49]	Shenyang Tonglian Group Co., Ltd./Chinese Academy of Medical Sciences	Phase III Clinical	
S-892216	Shionogi, Inc.	Phase III Clinical	
Pentarlandir UPPTA[50]	SyneuRx International Corp.	Phase II Clinical	
masitinib[51]	AB Science SA	Phase II Clinical	
EDP-235[52]	Enanta Pharmaceuticals, Inc.	Phase II Clinical	
PF-07817883[53]	Pfizer	Phase II Clinical	
NK01-63[54]	Sorrento Therapeutics, Inc.	Phase I Clinical	
ABBV-903	AbbVie	Phase I Clinical	
GS221	Grand Medical Pty, Ltd.	Phase I Clinical	
ASC-11	Clarion Biologicals	Phase I Clinical	

https://doi.org/10.1021/acsomega.4c03023
ACS Omega 2024, 9, 34196−34219

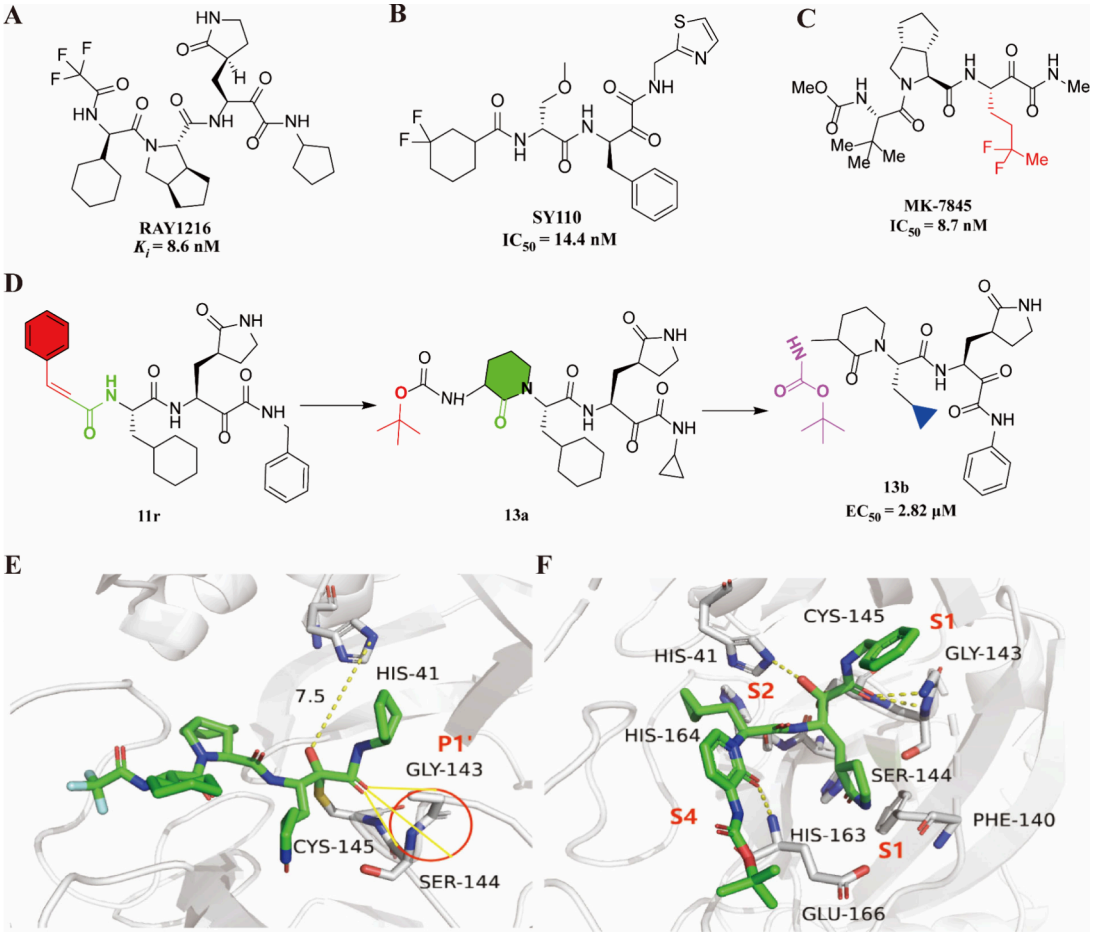

Figure 3. Molecular structure (A) and crystal structure (E) of **RAY1216** (PBD ID: 8IGN). The molecular structures of **SY110** (B) and **MK-7845** (C) (red color indicates the modified moiety at P1). The optimization process from **11r** to **13b** (D) and crystal structure of **13b** (F) (PBD ID: 6Y2F) (C) (Represent the evolution of **13b** in turn in red, green, purple, and blue.) (All structural formulas were drawn in ChemDraw; 3D representations were drawn in Pymol.)

with Phase III trials indicating its efficacy in treating mild to moderate SARS-CoV-2 infections, significantly shortening recovery times for patients with high viral loads without necessitating coadministration with ritonavir, thereby reducing medication risk and offering a superior treatment option for high-risk individuals.

Yang's team[57] identified four compounds that can inhibit the activity of M^{pro} by fluorescence resonance energy transfer (FRET) and structurally optimized Hit-1, the most potent of these compounds, to obtain **SY110** (Figure 3B). Strong in vitro antiviral efficacy was demonstrated against SARS-CoV-2 Alpha (B.1.1.7), Beta (B.1.351), and Omicron (B.1.1.529) BA.2 and BA.5 subspectra. Subsequent drug metabolism and pharmacokinetics of **SY110** were evaluated in beagle dogs, monkeys, and mice with oral utilization of 131.99%, 24.36%, and 67.42%, respectively. This was followed by an Ames mutagenicity assay, a chromosomal aberration assay, an hERG channel blocking assay, and a reproductive toxicity assay, which demonstrated that **SY110** has an excellent preclinical safety profile. The investigators also evaluated the in vivo antiviral activity of **SY110** in a K18-Hace2 transgenic mouse model infected with Omicron BA.2, which effectively inhibited the production of infectious viral particles in the lungs of the mice, and when **SY110** was coadministered with Ritonavir, it effectively inhibited Omicron infections in the airways and attenuated viral-induced lung lesions due to the virus. Unfortunately, the human liver microsome (HLM) stability of **SY110** still needs to be improved, but it is still a promising antiviral candidate.

Most SARS-CoV-2 M^{pro} covalent inhibitors reported contain amides as Gln mimics at P1. To develop a new inhibitor, Shurtleff's team[58] chose difluorobutyl as a substituent at this position, obtaining the compound **MK-7845** (Figure 3C). **MK-7845** was highly potent in vitro (IC_{50} = 8.7 nM in WT) and showed potent efficacy in an in vivo viral infection model. SAR analysis and X-ray crystallographic studies have shown that this moiety interacts with His163, which is the same residue that normally forms hydrogen bonds with the amide substituent found at P1. Compared to Nirmatrelvir, its physicochemical properties and preclinical pharmacokinetic profile facilitate easy-to-control predictive human oral dosing without the need for augmentation by CYP3A4 inhibition.

The group of Rolf Hilgenfeld[59] designed compounds containing an α-ketoamide moiety (**11r**), and it had excellent antiviral activity in Huh7 cells with MERS-CoV infection. They then optimized based on **11r** to obtain **13a**,[60] increasing the compound's half-life in plasma. To enhance the antiviral activity of the inhibitor, the researchers replaced the P2 cyclohexyl group of **13a** with the cyclopropyl group of **13b** (Figure 3D). Testing at the lung tissue level and observing the pharmacokinetics of **13b** revealed that it was well tolerated by inhalation and produced no adverse effects. This suggests that

https://doi.org/10.1021/acsomega.4c03023
ACS Omega 2024, 9, 34196−34219

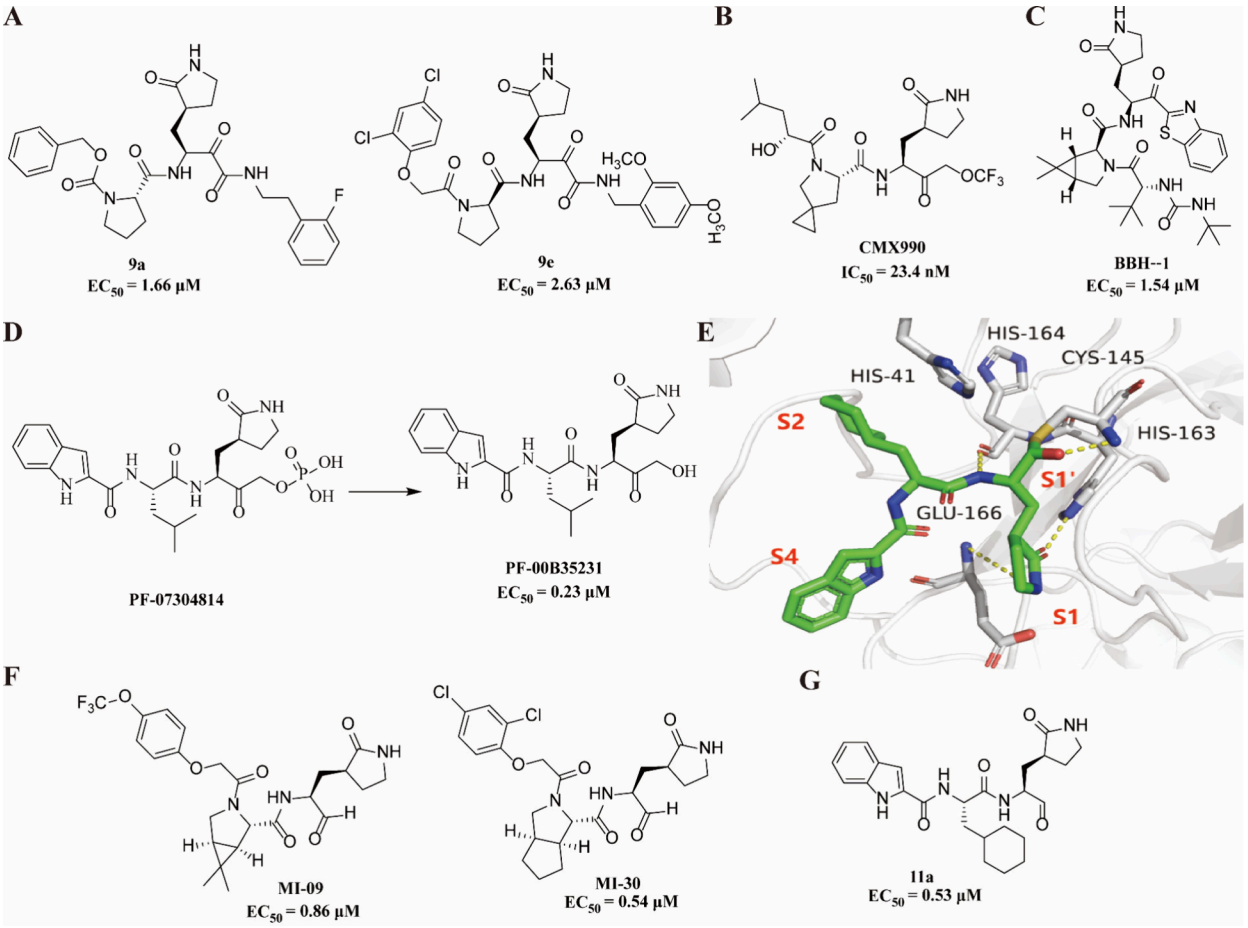

Figure 4. Molecular structures of **9a** and **9e** (A); the molecular structures of **CMX990** (B) and **BBH-1** (C); the molecular structures of **PF-07304814** and **PF-00835231** (D); the molecular structure (G) and crystal structure (E) of **11a** (PBD: 6LZE); and the molecular structures of **MI-09** and **MI-30** (F).

compound **13b** can be administered directly to the lungs. In addition, the group of Vincenzo Summa[61] synthesized a set of α-ketoamide derivatives via the PADAM (Passerini reaction−Amine Deprotection−Acyl Migration) strategy of α-hydroxy-β-aminoamides, confirming the affinity of the ketoamide fraction for covalent binding to the catalytic residue Cys145 of M^{pro}. Their crystalline structures show the possibility of inserting electron-withdrawing and -donating groups into the phenyl ring of the ketoamide moiety (Figure 3F). To predict their binding modes and mechanisms of action, the researchers performed molecular docking studies on key molecules **9a** and **9e** (Figure 4A) and demonstrated the expected formation of tetrahedral thiosemicarbazone adducts capable of mimicking the hydrolyzable amide bonds of natural substrates. Cellular experiments **9a** and **9e** showed the inhibitory potency of nanomolar and the potential of both to act as broad-spectrum coronavirus inhibitors. It certainly contributed to further research on SARS-CoV-2 inhibitors in humans.

PF-00835231, a standout in the category of peptidomimetic inhibitors, is an irreversible hydroxy ketone inhibitor targeting the SARS-CoV-2 main protease, evolved from its precursor **PF-07304814**[62] (Figure 4D). In vitro assays on renal cell lines revealed that its antiviral activity is notably enhanced (achieving an EC_{50} of up to 0.23 μM) when combined with a P-glycoprotein (P-gp) transporter protein blocker without exhibiting cytotoxicity. Additionally, **PF-00835231** presents a low risk of interactions with other drugs, which is attributed to its metabolic stability.

Building on **PF-00835231**, Damian W. Young's team[63] developed a compound with a trifluoromethoxymethyl ketone warhead, achieving an over 3-fold potency increase and significantly improved in vitro clearance (includes SARS-CoV-2 M^{pro} IC_{50}, HeLa-ACE2 CoV-2 $EC_{50/90}$, etc.). Through further experimentation with various P3−P2 combinations and incorporation of proline at P2, they identified **CMX990** as a clinical candidate (Figure 4B). This compound, distinguished by its α-hydroxy acid P2-cap and 4-spiral cyclopropyl proline at P2, exhibited no significant inhibition of major CYP isoforms, promising oral bioavailability and tolerability in preclinical species. With its innovative covalent warhead, **CMX990** exhibited remarkable antiviral properties (IC_{50} = 23.4 nM) and low projected human clearance. This compound swiftly progressed to Phase 1 clinical trials in just around 10 months, showcasing rapid advancements in peptidomimetic inhibitor development.

3.1.2. Aldehyde-Containing Inhibitors. Dai's team[64] synthesized an aldehyde, **11a** (Figure 4G), which exhibited significant anti-SARS-CoV-2 infection activity against SARS-CoV-2-M^{pro} with EC_{50} of 0.53 Mm, respectively. In multiple variants of in vitro treatment of infections, the best compound **11a** showed good activity against omicron (EC_{50} = 0.26 μM), delta (EC_{50} = 0.027 μM), beta (EC_{50} = 20.28 μM), and alpha (EC_{50} = 3.39 μM) and no significant cytotoxicity.[48] Crystallo-

https://doi.org/10.1021/acsomega.4c03023
ACS Omega 2024, 9, 34196−34219

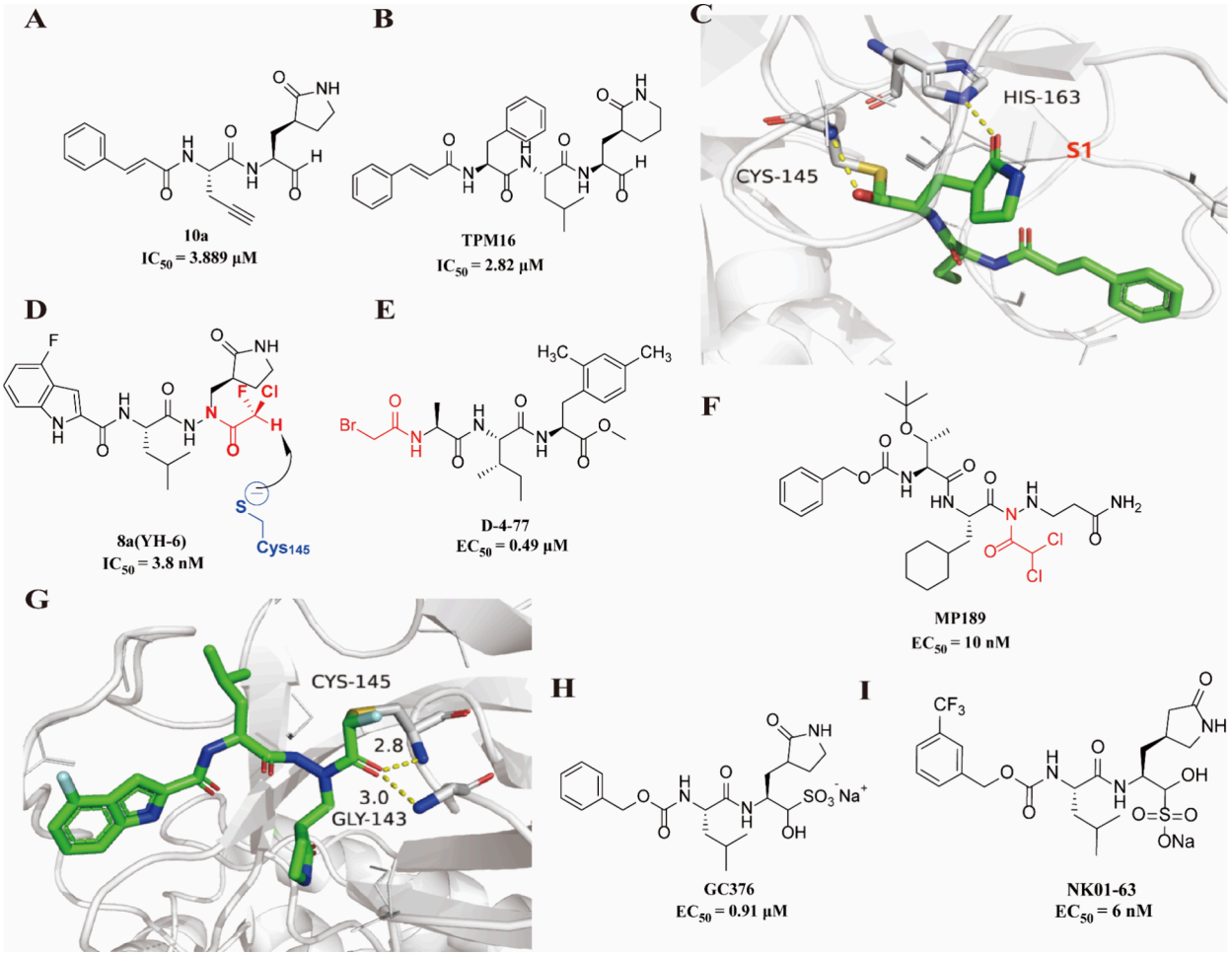

Figure 5. Molecular structure (A) and crystal structure (C) of **10a** (PBD: 7DHJ). The molecular structures of **TPM16** (B). The molecular structure (D) and crystal structure (G) of **YH-6** (PBD: 7XAR). The molecular structure of **D-4-77** (E) and **MPI89** (F) (the warheads of **YH-6**, **D-4-77**, and **MPI89** are marked in red). The molecular structure of **GC376** (H) and **NK01-63** (I).

graphic study of **11a** shows that the amide bond on the **11a** chain makes a hydrogen bridge with His164, and the P3 indole group is exposed at the S4 site and makes a hydrogen bridge with Glu166. Its lactam ring amide group H-bonds with His163, and its cyclohexyl moiety **11a** at P2 enters the S2 site and overlaps with the His41 imidazole nucleus. The oxygen atom of this aldehyde group H-bonds to the backbone of residue Cys145 via the S1 position, which has a key effect in orienting the conformation of the inhibitor (Figure 4E). Currently, **11a** is a promising broad-spectrum drug inhibitor, and it is being further investigated in the form of inhalation nebulization. Of these, **11a** (Clinical Trial Number: FB2001) has shown safety and tolerance in a first-in-human study in the US and is entering a Phase III clinical trial in the Chinese population.

Yang et al. conceived and prepared 32 bicyclo proline analogs based on boceprevir and telaprevir, of which **MI-09** and **MI-30** (Figure 4F) showed the most potent inhibitory effect against SARS-CoV-2-M^{pro}.[65] **MI-09** and **MI-30** use aldehydes as P1 warheads, which bind covalently to the catalytic site Cys145 and promote the molecules' antiviral activity. Evaluation of SARS-CoV-2 infected VeroE6 cells showed that **MI-09** and **MI-30** had outstanding inhibitory activity with an EC_{50} of 0.86 and 0.54 μM, respectively. In a murine model of SARS-CoV-2 disease, intravenous **MI-09** and **MI-30** were not significantly toxic to mice and efficiently inhibited SARS-CoV-2 multiplication and reduced the area of lung lesions caused by SARS-CoV-2 in vivo. In addition, both have shown excellent pharmacokinetic characteristics and a safe efficacy in rats.

Shang's team[66] reported the design and synthesis of a series of peptidomimetic compounds, of which compound **10a** (Figure 5A) showed significant inhibitory activity to SARS-CoV-2-M^{pro} with IC_{50} levels of 3.889, respectively. Crystallographic studies revealed that the aldehydic group of **10a** binds covalently to Cys145, and the γ-lactam nucleus interacts with hydrogen with His163 and associates with the S1 pocket of M^{pro} (Figure 5C), reflecting the tightness of the binding between the molecule and M^{pro} and indicating that the mimetic class of inhibitors still has much to be investigated.

Based on the lead compound **13b**,[60] the investigators used a tetrapeptide simulation approach to design **TPM16** (Figure 5B).[67] It showed a potent inhibitory effect on SARS-COV-2-M^{pro} (IC_{50} = 0.16 μM). The EC_{50} in the VeroE6 cell line was 2.82 μM. In addition, the inhibitor was not significantly toxic in the cell toxicity assay (CC_{50} > 200 μM). Its structural analysis indicated that **TPM16** was successfully bound to the dimeric histidine residue (His41) of M^{pro} and attenuated the cellular viral burden of SARS-CoV-2, providing the basis for

https://doi.org/10.1021/acsomega.4c03023
ACS Omega 2024, 9, 34196−34219

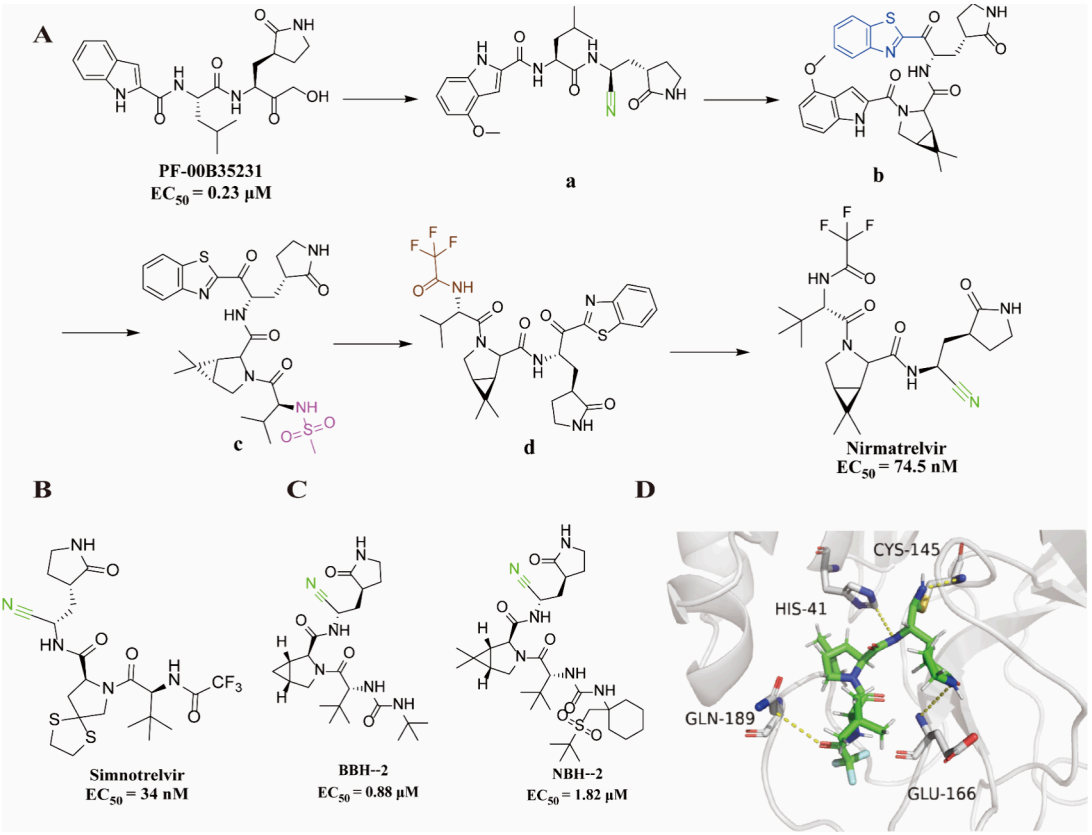

Figure 6. Molecular structure of **Nirmatrelvir** and its base structure (A) (different colors mark the main variations of the compounds). The crystal structure of **Nirmatrelvir** (D) (PBD: 7RFS). The molecular structure of **Simnotrelvir** (B) (nitrile groups are shown in green). The molecular structure of **BBH** series (C).

the future development and optimization of various antiviral protease inhibitors.

3.1.3. Haloacetyl-Containing Inhibitors. The inhibition mechanism of compounds with halogenated warheads involves a nucleophilic attack on the C−X bond by cysteine-SH, leading to the formation of an irreversible S−C bond. Recently, there has been significant research on this class of inhibitors, focusing on α-haloacetamides, α,α-dihaloacetamides, and α,α,α-trihaloacetamides as reactive groups.[68,69]

YH-6 (**8a**, Figure 5D), a class of covalent inhibitors targeting M^{pro},[70] effectively inhibited SARS-CoV-2-M^{pro} at the nM level (IC_{50} = 3.8 nM), showing promising activity. It also showed little toxicity in 293T-VeroE6 cells (CC_{50} > 35 μM). The protein and **YH-6** complex crystal structure showed that chlorofluoroacetamides (CFA) of **YH-6** covalently bind to Cys145 at the active site; in the oxygen anion pore, the carboxylic acid amide oxygen of the CFA moiety forms two hydrogen bonds with the Gly143 residue and the NH group of the Cys145 backbone, which may be essential for the stabilization of the covalent bond with the Cys145 residue (Figure 5G). These results indicate that **YH-6** has antiviral activity at the nM level and good pharmacokinetic properties and is a potential lead compound for use as a COVID-19 therapeutic agent.

Current studies on drug development targeting SARS-CoV-2 M^{pro} have focused on the S4−S1′ site in its substrate binding pocket. To increase the diversity of SARS-CoV-2-M^{pro} inhibitors, Liu's team[71] developed novel SARS-CoV-2 M^{pro} covalent inhibitors targeting the S1′−S3′ sites. By exploring the substrate selectivity of the S1′−S3′ sites, the researchers found that the S1′ site prefers Ala, S2′ prefers Lys/Ile, and S3′ prefers Phe/Trp and that the S1′−S3′ pockets of M^{pro} have a high affinity for the peptide sequence Ala-Ile-Phe (AIF). Therefore, they designed and synthesized the best active inhibitor, **D-4-77**, using AIF as the backbone and bromoacetamide as the covalent warhead (Figure 5E). **D-4-77** showed excellent antiviral efficacy (EC_{50} = 0.49 μM) in Vero E6 cells infected with SARS-CoV-2. Next, the researchers found that **D-4-77** can restore the host NF-κB immune response by inhibiting M^{pro}, so **D-4-77** can not only inhibit the replication of SARS-CoV-2 but also be an immunoprotectant against the damage of the innate immune response caused by SARS-CoV-2. Although the **D-4-77** series of inhibitors has not yet been studied in animal or clinical studies, the studies described above demonstrate the effectiveness of the S1′−S3′ pocket of M^{pro} in the study of inhibitors. Therefore, the study of **D-4-77** could provide a new direction for subsequent inhibitor research.

Khatua's team[72] explored the inhibitory effect of azapeptides in combination with various covalent warheads on SARS-CoV-2. They obtained the most available compound, **MPI89**, featuring an azido-2,2-dichloroacetyl warhead (Figure 5F). In ACE2 A549 cells, **MPI89** showed potent inhibition of SARS-CoV-2 (EC_{50} = 10 nM). Crystallographic analysis showed that these inhibitors covalently bind Cys145 and use the azamido carbonyl oxygen to bind to the oxygen anion cavity.

3.1.4. Water-Soluble Aldehyde Bisulfite Adducts. **GC376** is a dipeptide bisulfite that inhibits some small RNA viruses and coronaviruses (Figure 5H). **GC376** was converted to **GC373** in vivo after administration, thus inhibiting viral replica-

https://doi.org/10.1021/acsomega.4c03023
ACS Omega 2024, 9, 34196−34219

tion.[73−77] Studies have shown that **GC376** successfully reverses experimentally induced FIP (feline infectious peritonitis) and naturally occurring FIP in cats, suggesting that **GC376** inhibits coronavirus infection in vivo.[78] Xu's group[74] treated VeroE6 cells infected with SARS-CoV-2 with **GC376** and observed protection against cytopathic effect (CPE) and a dose-dependent decrease in viral CPE with an EC_{50} of 0.91 μM, allowing further development into a broad-spectrum anticoronaviral agent.

Brent R. Stockwell's group[54,79] identified **NK01-63** as the most promising of these compounds during the optimization of **GC376** analogues and named it coronastat. The investigators tested the binding selectivity of **NK01-63** to human proteases and found that **NK01-63** was consistently more selective than the human protease chymotrypsin for SARS-CoV-2-M^{pro} and highly selectively inhibited M^{pro} (Figure 5I). **NK01-63** consistently exhibited excellent antiviral potency in human Huh-7 cells, EC_{50} = 146 nM. **NK01-63** could effectively block the replication of human coronavirus alpha OC43 and human coronavirus beta 229E with EC_{50} < 100 nM in Huh-7 cells. The investigators then conducted in vivo toxicity and pharmacokinetic studies of **NK01-63** using C57BL/6 mice, which showed that **NK01-63** was not toxic in vivo by any of the routes of administration, and the concentration of **NK01-63** in the lungs of the mice was still higher than its EC_{90} value at 24 h postdose. Therefore, preclinical studies of **NK01-63** are expected to be conducted to evaluate its potential for clinical development. It is currently in clinical phase I.

3.1.5. Nitrile-Containing Inhibitors. Nitrile warheads play a crucial role in the study of M^{pro} inhibitors. Due to its different electronegativity from the nitrogen atom, the carbon atom of the nitrile is more susceptible to protease-catalyzed nucleophilic addition of cysteines to form reversible covalent adducts of thiosemicarbazide esters.[80] In addition, the electron-attracting nature of the nitrile groups can alter the reactivity of the surrounding molecules, contributing to the functionalization of adjacent positions.

To address **PF-00835231**'s limited bioavailability, researchers modified its structure by replacing the hydroxymethyl ketone group with a cyano group, resulting in **Compound a**[29] (Figure 6A). This alteration improved oral bioavailability in rat models, albeit with a reduction in efficacy and antiviral potency against SARS-CoV-2 M^{pro}. Further structural adjustments led to **Compound b** (Figure 6A), which incorporated 6,6-dimethyl-3-azabicyclo[3.1.0]hexane at the P2 site and featured a benzothiazole-2-yl ketone warhead, enhancing its permeability but compromising potency and metabolic stability. The introduction of a methanesulfonamide group at the P3 position in **Compound c** elevated its hydrogen bond affinity with Glu166, improving both potency and antiviral activity (Figure 6A). The quest for enhanced antiviral activity led to the development of **Compound d** (Figure 6A), which included a trifluoroacetamide group at P3. This backbone, when combined with a nitrile warhead, resulted in the creation of **Nirmatrelvir**, a potent inhibitor against SARS-CoV-2 M^{pro} with significant antiviral efficacy (Figure 6A, D). Given **Nirmatrelvir**'s susceptibility to rapid metabolism by the CYP3A4 isoenzyme, it is coadministered with **Ritonavir**, a CYP3A4 inhibitor, to prolong its activity and maintain higher concentrations in vivo.[81] This combination, known as **Paxlovid**, was authorized on December 27, 2021, for treating adults and adolescents with mild to moderate COVID-19, significantly reducing the risk of severe illness by 89% compared to a placebo without notable safety concerns. **Paxlovid** has received widespread approval for treating severe COVID-19 in adults not requiring oxygen supplementation.[30,31]

However, the researchers found that the T21I (S4′ subsite)/E166V (S1 subsite) and L50F (S2 subsite)/E166V mutants of M^{pro} increase the enzymatic activity of the protease by directly decreasing the binding affinity of SARS-CoV-2 to nirmatrelvir (**Ensitrelvir** has a similar resistance pattern).[82] Although current clinical data indicate that nirmatrelvir remains consistently effective against the most recent omicron variants,[83] it is imperative to monitor closely for amino acid mutations and secondary adaptive mutations that confer resistance to nirmatrelvir in the future. It may be beneficial for investigators to consider inhibiting M^{pro} activity through combination therapy (e.g., a mixture of a M^{pro} inhibitor, a PL^{pro} inhibitor, and an RdRp inhibitor) or other specific binding strategies that do not require binding to any of the subsites of **Nirmatrelvir** (e.g., natural inhibitors).[84] If small-molecule compounds that bind differently to the M^{pro} catalytic site are developed in the future, they will be more effective in treating COVID-19 and preventing the rise of SARS-CoV-2 resistance.[35,85]

Xu and colleagues[36−38] obtained the oral clinical candidate **Simnotrelvir** (Figure 6B) by stepwise optimization of P1, P2, and P4 based on the boceprevir warhead. Among them, the biophysical, structural, and biochemical data of **Simnotrelvir**, as well as its effective covalent binding to the SARS-CoV-2-M^{pro} active site, provide a solid structural basis for anti-SARS-CoV-2. Researchers then performed in vivo pharmacokinetic characterization of **Simnotrelvir** in rats (15 mg/kg IV, 15 mg/kg PO) and monkeys (5 mg/kg IV, 5 mg/kg PO), with 35.3% of rats and 41.9% of crab-eating monkeys showing good oral bioavailability. Next, the investigators evaluated the selectivity of **Simnotrelvir** for human proteins, its toxicity to human peripheral blood mononuclear cells (PBMCs), to human hepatocytes, as well as to rats and monkeys, all of which demonstrated that **Simnotrelvir** was well-tolerated and safe in vivo. The in vivo antiviral activity of **Simnotrelvir** was evaluated in a K18-Hace2 transgenic mouse model, and it was found that **Simnotrelvir** protects mouse lung and brain tissues from lesions and that there is a good correlation between drug exposure and in vivo antiviral efficacy for the combination of **Simnotrelvir** and ritonavir. Meanwhile, **Simnotrelvir** was launched on January 29, 2023, in China.

BBH-1, **BBH-2**, and **NBH-2** (Figures 4C and 6C) are a series of reversible covalent inhibitors targeting M^{pro} designed by Andrey Kovalevsky et al.[86] The structure of this class contains an electrophilic ketone slug that covalently binds to Cys145 to produce a hemithioketal, which facilitates the tight association of the compound with M^{pro}. The crystalline structure resulting from the complex of M^{pro} with **BBH-1** suggests that the reaction between Cys145 at the S1′ position and the ketone group of this inhibitor generates an oxygen anion, which facilitates the creation of hydrogen bridges and, hence, the stabilization of the molecule. The results of the **BBH-1**, **BBH-2**, and **NBH-2** antiviral activity in Vero E6 TMPRSS cells showed that this class of compounds had a significant antiviral effect showing an EC_{50} of 1.54, 0.88, and 1.82 μM, respectively, only slightly lower than that for **PF-07321332** (EC_{50} = 0.25 μM).

https://doi.org/10.1021/acsomega.4c03023
ACS Omega 2024, 9, 34196−34219

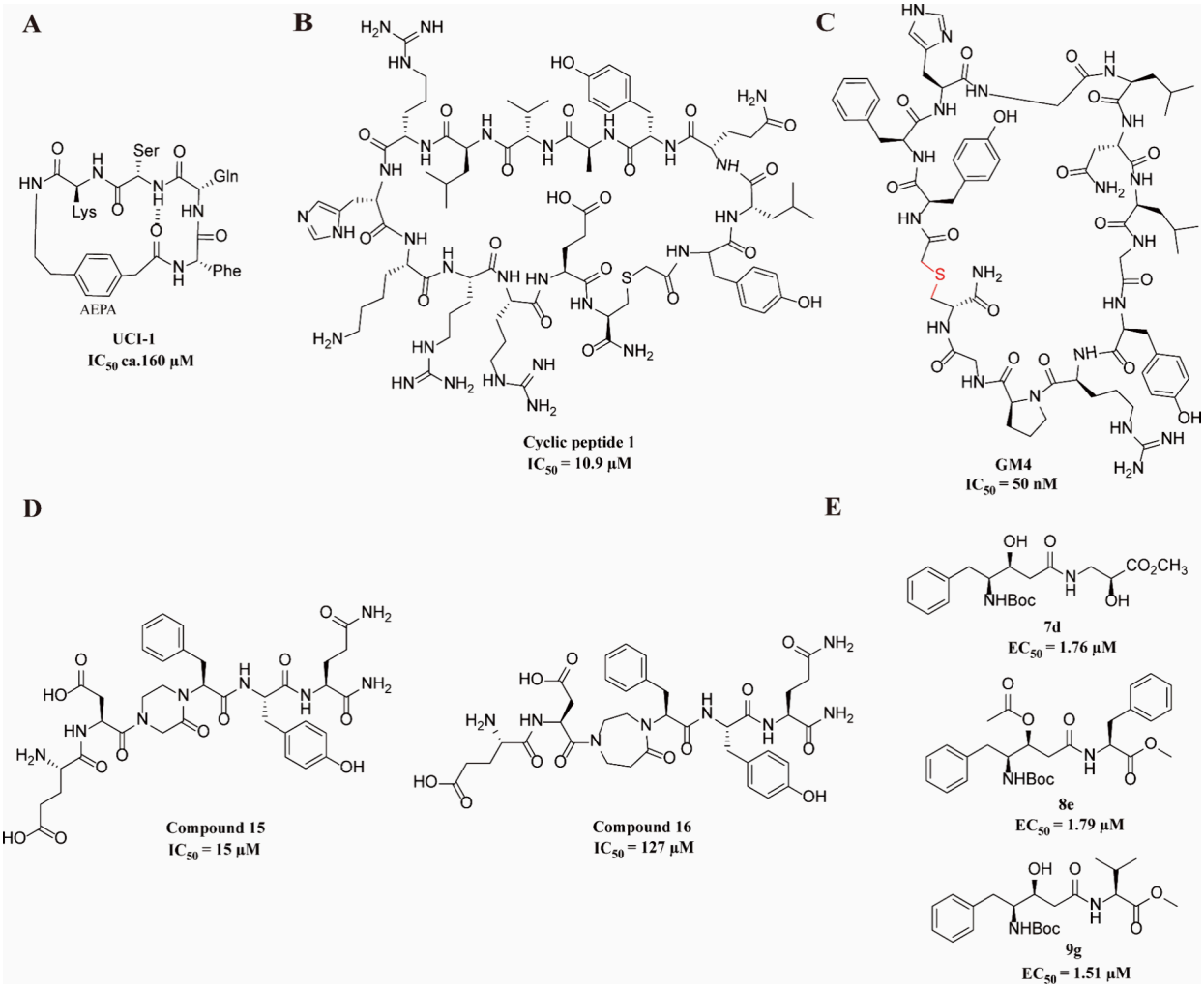

Figure 7. Molecular structure of **UCI-1** (A), **Cyclic peptide 1** (B), **GM4** (C) (the ring-forming portion is shown in red), **Compound 15** and **Compound 16** (D), and **7d**, **8e**, and **9g** (E).

3.1.6. Cyclic Peptide Inhibitors. Currently, most of the research on M^{pro} inhibitors is done with linear analogs.[87,88] The conformational stability and biological activity of cyclic peptides often show significant advantages over linear analogs. At the same time, this structural elephantine rigidity of the cyclic peptide itself increases resistance to degradation by endogenous proteases, thus further improving plasma stability.[89]

UCI-1[90] is a cyclic pentapeptide, a cyclic peptide inhibitor that generates M^{pro} directly from the crystal structure of a linear peptide substrate (Figure 7A). Its structure is characterized mainly by the addition of a methylene group to the para-position of Phe309 of the linear peptide substrate, which is then linked to the backbone carbonyl of Phe305 and finally to the [4-(2-aminoethyl) phenyl]-acetic acid (AEPA) moiety to form a rigid peptide macrocycle. This structure is analogous to the conformation of the C-terminal autolytic cleavage site of the naturally occurring M^{pro} substrate. In the enzyme inhibition assay, the IC_{50} of **UCI-1** was about 160 μM, which showed a certain inhibitory effect at a micromolar concentration. In HEK-293 cells, **UCI-1** was not cytotoxic at concentrations up to 256 μM. Although UCI-1 is not particularly active, it provides a foundation for the development of additional cyclic peptide inhibitor analogs with enhanced M^{pro} activity.

Payne's team[91] used the random nonstandard peptide integrated discovery (RaPID) technique to obtain the SARS-CoV-2 M^{pro} target thioether-linked **Cyclic peptide 1** (Figure 7B). Based on multiangle laser light scattering with size exclusion chromatography (SEC-MALLS) and nuclear magnetic resonance (NMR) data, **Cyclic peptide 1** selectively binds and inhibits the active homodimer of the SARS-CoV-2 M^{pro} active homodimer but not the inactive monomer. In vitro assessment of inhibitory activity showed that at a concentration of 10 μM **Cyclic peptide 1** was inactive against MERS-CoV M^{pro}, SARS-CoV-2 PL^{pro}, TMPRSS2, furin, and cathepsins B and E, and it moderately inhibited histone L (IC_{50} = 10.9 μM). It has a high stability in human plasma with a residual rate of 85% after 24 h. It was inactive at a concentration of 50 μM in the antiviral activity assessment, but when combined with cell-penetrating peptide (CPP), it enhanced cellular uptake and significantly improved antiviral activity. This indicates that **Cyclic peptide 1** has the potential to be an effective antiviral agent when coupled with CPP.

The research team led by Hiroaki Suga[92] discovered that **GM4** and **GM4H3Q** are highly potent cyclic peptides that specifically target the M^{pro} enzyme (Figure 7C). Initially, the

https://doi.org/10.1021/acsomega.4c03023
ACS Omega 2024, 9, 34196−34219

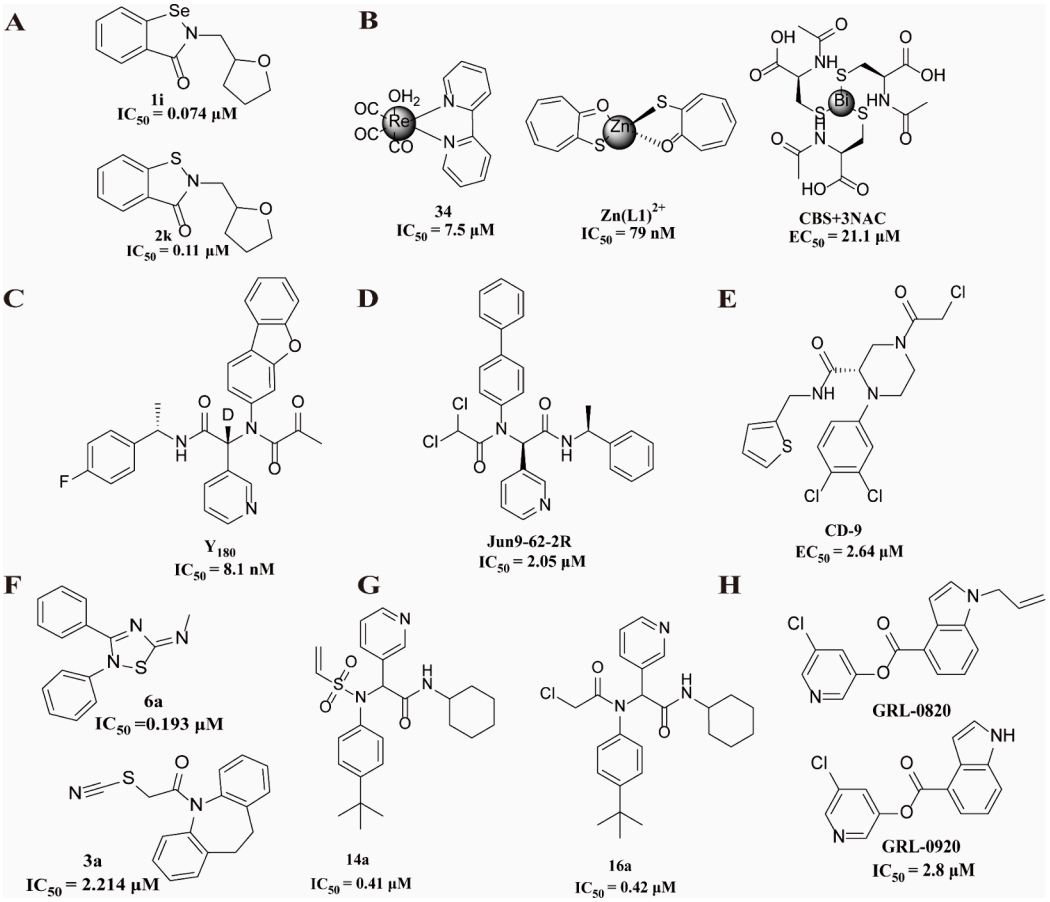

Figure 8. Molecular structure of **1i** and **2k** (A), metal complexes (B), **Y180** (C), **Jun9-62-2R** (D), **CD-19** (E), **6a** and **3a** (F), **16a** and **14a** (G), and **GRL-0820** and **GRL-0920** (H).

researchers constructed a comprehensive cγAA macrocyclic peptide library. From this library, they identified seven macrocyclic peptides containing cγAA that exhibited a strong binding affinity, inhibitory activity, and protein hydrolysis stability. Notably, **GM4**, which incorporates γ1, demonstrated an exceptional K_d value of 5.2 nM, surpassing **GM2**, which shared the same motif but had a K_d value of 71 nM. Employing an ms-based approach, the researchers evaluated the inhibitory effect of **GM1** to **GM7** on M^{pro}. Among these peptides, GM1, GM4, and GM5, which share the yFHγX motif, exhibited impressive IC_{50} values of 40, 50, and 40 nM, respectively. Furthermore, when the team assessed the half-life of this effective cγ aa-containing peptide and their mutants in human serum, **GM1**, **GM4** (containing γ1), and **GM5** (containing γ2) demonstrated remarkable resistance to peptidase degradation. Specifically, these peptides had half-life ($t_{1/2}$) values of 90, 126, and 32 h, respectively. The presence of the yFH motif in **GM4** appears to contribute significantly to its high potency and stability, making it a promising candidate for further inhibitor research and development.

3.1.7. Other Inhibitors. By drawing on the development of molecules targeting protein−protein interactions (PPIs), Trabocchi's group[93] was able to develop a molecule capable of inhibiting SARS-CoV-2 ACE2/spiny interactions in the micromolar range, **Compound 15** and **Compound 16** (Figure 7D). It was obtained through the researchers' synthesis within a few steps using iminium chemistry. Both compounds were successfully incorporated into the short peptide epitope EDLFYQ of the ACE2 α-helix 1 structural domain. This demonstrated that they inhibited the ACE2/spike interaction of SARS-CoV-2 in the micromolar range (IC_{50} values of 15 ± 6 and 127 ± 76 μM, respectively). Using the ACE2 epitope and the c-terminal Q amino acid present in the M^{pro} recognition motif, the investigators assessed the inhibitory effect of the synthesized mimetic peptide on the main protease activity of SARS-CoV-2 M^{pro}. This approach provides a new avenue for developing multitargeted therapeutic agents against coronavirus infections.

In addition, Azevedo's team[94] worked on peptidomimetic analogs of statins (**7d**, **8e**, and **9g**) (Figure 7E). The three most potent compounds (**7d**, **8e**, and **9g**) inhibited M^{pro} activity in the submicromolar range and were not cytotoxic, inhibiting about 80% of SARS-COV-2 replication. Molecular dynamics simulations further confirmed the stability and persistent interaction of the compounds binding to the M^{pro} site.

3.2. Nonpeptidomimetic Inhibitors. Nonpeptidomimetic inhibitors, primarily originating from high-throughput screening, are categorized as either covalent or noncovalent inhibitors. These inhibitors have demonstrated favorable oral bioavailability and prolonged half-lives, suggesting enhanced in vivo efficacy and decreased potential for drug interactions.[95,96]

3.2.1. Covalent Inhibitors. **Ebselen** is a class of small-molecule organoselenium compounds that were found to be effective in inhibiting SARS-CoV-2-M^{pro} (K_i = 2 μM, IC_{50} = 0.67 μM) and showed potent antiviral effects on SARS-CoV-2 infected Vero cells by Jin et al. in 2020 (EC_{50} = 4.67 μM).[97] In the **Ebselen**-M^{pro} complex, **Ebselen** can form covalent bonds with Cys145 and Cys44 of M^{pro}.[98] On this basis, the Sun's

https://doi.org/10.1021/acsomega.4c03023
ACS Omega 2024, 9, 34196−34219

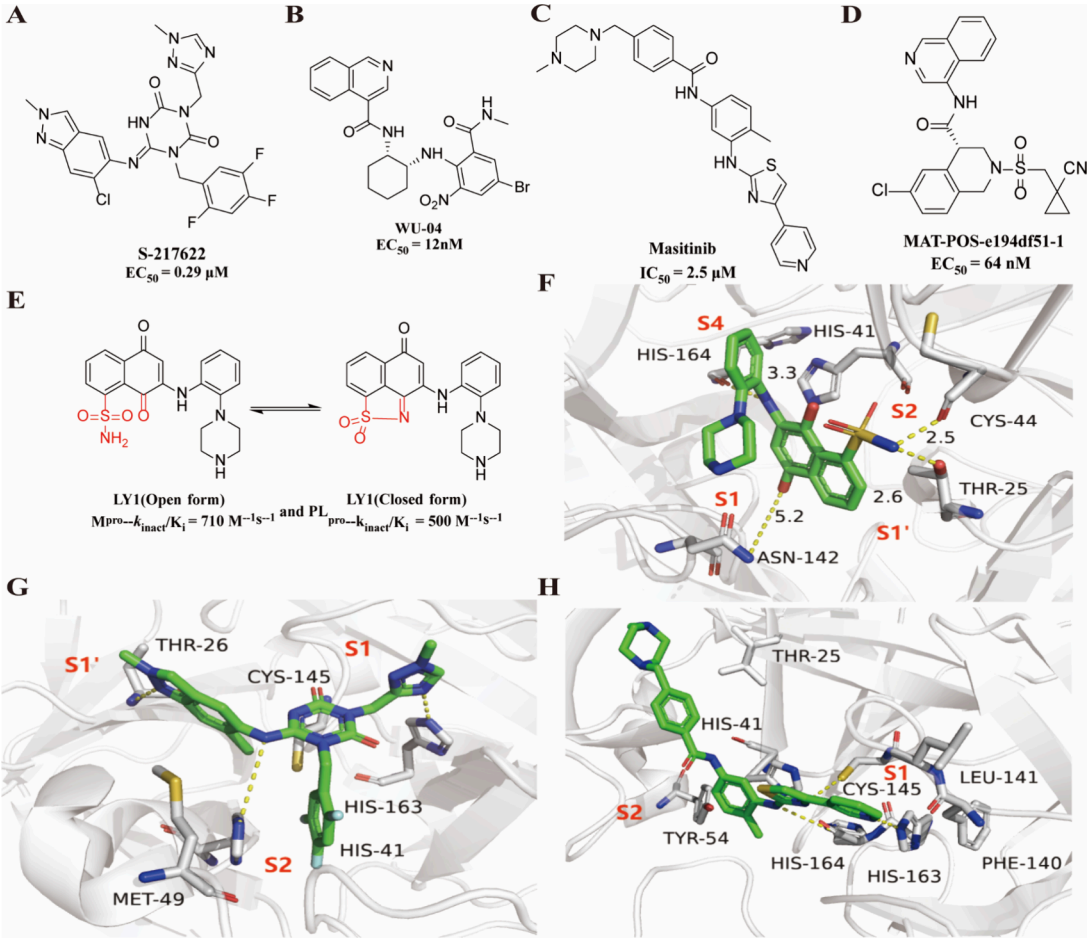

Figure 9. Molecular structures (A) and crystal structure (G) of **S-217622** (PBD: 7VU6). The molecular structure of **WU-04** (B). The molecular structure (C) and crystal structure (H) of **Masitinib** (PBD: 7JU7). The molecular structure of **MAT-POS-e194df51-1** (D). The molecular structure (E) and crystal structure (F) of **LY1** (PBD: 7V1T) (the differences between the two forms of LY1 are marked in red).

group[99] tested the inhibitory effect of **Ebselen** and **Ebsulfur** derivatives, of which **1i** and **2k** (Figure 8A) showed better enzyme inhibition than **Ebselen** with IC_{50} values of 0.074 and 0.11 μM, respectively. However, DTT-dependent inhibition assays indicate that **Ebselen** and **Ebsulfur** are promiscuous cysteine protease inhibitors of M^{pro}. Deval et al.[100] questioned the role of **Ebselen** as a protease inhibitor, finding that **Ebselen** did not inhibit SARS-CoV-2 replication but was toxic to Vero cells. Subsequently, Wang's team[101−103] demonstrated that **Ebselen** is not a specific M^{pro} inhibitor. The study revealed that **Ebselen** had no inhibitory effect in either the FlipGFP assay or the Protease-Glo luciferase assay.

Metal complexes also have inhibitory activity against SARS-CoV-2-M^{pro}, for example, competitive Hg^{2+} and Zn^{2+} coupling inhibitors. Karges[104] prepared and tested a series of Re1-tricarbonyl complexes in which the ligand covalency of a single Re1 could bind the tricarbonyl complex and thus inhibit the action of M^{pro}. Enzymatic activity assays demonstrated that these complexes exhibit IC_{50} values below 10 μM, with **Compound 34** (Figure 8B) displaying the highest activity. Additionally, zinc ions have been shown to block the replication of SARS-CoV-2 in the micromolar range with limited cellular toxicity.[105,106] The bismuth ion, a fringe metal ion that binds cysteine, has also been explored. One analog, colloidal bismuth subcitrate (**CBS**), combined with *N*-acetyl-L-cysteine (**NAC**), inhibited the M^{pro} with an IC_{50} of 22.25 μM[107] (Figure 8A). Currently, phase III clinical trials are ongoing for oral bismuth-containing drugs, including CBS, for the treatment of COVID-19.

Y180 (Figure 8C), a diamide derivative designed and synthesized by Quan's group,[108,109] exhibits remarkable antiviral activity against SARS-CoV-2 and its variants, including B.1.1.7 (Alpha), B.1.617.1 (Kappa), and P.3 (Theta). In vitro tests conducted in VeroE6 cells and the human lung epithelial cell line Calu3 demonstrated their efficacy in inhibiting virus replication. Furthermore, in the K18 transgenic mouse model expressing human angiotensin-converting enzyme 2 (K18-hACE2),[110−112] **Y180** exhibits potent antiviral activity with EC_{50} values in the nanomolar range for multiple virus variants. These findings suggest that **Y180** can effectively block virus replication, minimize tissue damage, and enhance survival rates in infected animals. Additionally, **Y180** demonstrates good oral bioavailability in mice, rats, and dogs, indicating its potential for oral administration. However, preclinical safety evaluation raises concerns regarding its toxicity, necessitating further investigation of its safety profile in humans.

Jun9-62-2R (Figure 8D) was obtained by ref 69 as an improvement on **23R** and is highly selective for M^{pro}. **Jun9-62-2R** was applied to Caco2-hACE2 cells infected with SARS-CoV-2 and showed good antiviral activity and no cytotoxicity (EC_{50} = 2.05 μM, CC_{50} > 100 μM). The crystal structure of

https://doi.org/10.1021/acsomega.4c03023
ACS Omega 2024, 9, 34196−34219

the complex of **Jun9-62-2R** with M^{pro} shows that the pyridine ring of **Jun9-62-2R** binds to the S1 site of M^{pro} and forms a hydrogen bond with His163, which is essential for the coordination of its basal Gln side chain. Partial insertion of **Jun9-62-2R** into the hydrophobic S2 pocket forms a nonpolar contact and stacks with the catalytic base His41. The amide group linking the pyridine ring to α-methylbenzene interacts with the hydrogen bond of the Glu166 backbone, helping the α-methylbenzene group to flip down into the core of the substrate channel and interact with the biphenyl moiety as a way of maximizing the effect of the inhibitor.

GD-9 is a nonmimetic class of covalent inhibitors using cysteine as a targeting warhead[113] (Figure 8E). The researchers tested the antiviral effect of **GD-9** in Vero E6 cells with an EC_{50} value of 2.64 μM and tested its toxicity with a CC_{50} = 12.5 μM, indicating that the molecule is somewhat toxic. The enzymatic kinetic and MALDI-TOF-MS studies indicate that **GD-9** is an irreversible covalent inhibitor of SARS-CoV-2 M^{pro} with a good affinity for M^{pro}. At the same time, **GD-9** has fewer side effects as it shows target selectivity toward coronavirus proteases. Therefore, addressing the toxicity of **GD-9** is a prerequisite for its further development as a clinical candidate for the therapy of COVID-19.

Ren's team[114] discovered a series of 2,3,5-substituted [1,2,4]thiadiazole analogs that act as nonmimetic covalent inhibitors of M^{pro}, demonstrating promising inhibitory activity at the molar level. To further explore the efficacy of these inhibitors, they focused on compound **6a** (Figure 8F). Using the FRET protease assay, they determined that compound **6a** exhibited an IC_{50} of 0.193 μM. Analysis of the frontier molecular orbitals (FMOs) and the molecular electrostatic potential (MEP) of **6a** indicated that the 2,3,5-substituted [1,2,4]-thiadiazole moiety has the potential to serve as a covalent warhead, thereby enhancing its inhibitory activity against M^{pro}. Based on the above, they also designed and synthesized inhibitor **3a**[115] using a scaffold hopping strategy with thiocyanate as a covalent warhead (Figure 8E). At the enzyme level, it showed good activity with an IC_{50} of 2.214 μM. The mechanism of action showed that compound **3a** binds tightly to the active pocket of M^{pro} while forming a disulfide bond with Cys145. Its carbonyl group formed a hydrogen bond with M^{pro} through water. At the S1′ and S2 sites, the tricyclic moiety by **3a** occupies these sites by interacting with His41, Met49, and Met165. Thus, this novel skeleton can be a probe molecule for future covalent chemistry. To some extent, this provides a new direction for the research and development of drugs targeting M^{pro} or other covalent drug candidates.

Based on compound X77, Nicolas Moitessier's team[68] used the Fitted docking technique, replacing the **X77** reactive group with an imidazole ring to form a hydrogen-bonding interaction with the backbone of Gly143, which increased the inhibitor's potency against the virus. Subsequently, the inhibitors **16a** and **14a** (Figure 8G) were assayed for activity at the enzyme level (IC_{50} values of 0.42 and 0.41 μM, respectively) and shown to be more potent than **X77** (IC_{50} = 4.1 μM).

Hattori's team[116] found that the indole-chloropyridyl ester derivatives **GRL-0820** and **GRL-0920** (Figure 8H) also exhibited inhibitory activity against SARS-CoV-2, particularly GRL-0920, which effectively blocked SARS-CoV-2 infection and cytopathic lesions (EC_{50} = 2.8 μM) with low toxicity.[117−119] In addition, the ketal covalently bound to **GRL-0920**-M^{pro} may be reversibly converted to a carbonyl group that is not covalently bound to M^{pro}. Therefore, it is unlikely that **GRL-0920** and its analogs will interact covalently to cause severe toxicity. These need to be further investigated and validated.

3.2.2. Noncovalent Inhibitors. **S-217622** (Figure 9A), also called **Ensitrelvir**, is a nonpeptide oral medicine approved for marketing in Japan on November 22, 2022. **Ensitrelvir** has antiviral activity against all variants of SARS-CoV-2 and inhibits viral replication by inhibiting M^{pro} protease activity. It also shows good pharmacokinetic properties when administered orally once a day in humans. The half-maximal inhibitory concentrations (EC_{50}) of **Ensitrelvir** in monkey kidney cells (Vero E6) expressing human transmembrane serine protease (TMPRSS2) against wild-type (WT), gamma, beta, alpha, and omicron variants of SARS-CoV-2 were 0.37, 0.33, 0.40, 0.50, and 0.29 μmol/L, respectively.[39] Most importantly, **Ensitrelvir** is highly bioavailable orally and has a prolonged half-life in vivo. The crystal structure of the complex of **Ensitrelvir** with M^{pro} shows that at the S1 site the 1-methyl-1*H*-1,2,4-triazole unit forms a hydrogen binding with NH of the side chain of His163. In the **Ensitrelvir** complex, their interaction maintains the His41 flipping feature, and the 2,4,5-trifluoromethyl portion of **Ensitrelvir** dominates the hydrophobic S2 pocket with overlapping His41 side chains. The P1′ ligand 6-chloro-2-methyl-2*H*-indazole fraction holds a hydrogen phase link with the Thr26 backbone NH and contacts Met49 hydrophobically (Figure 9G). In Phase II/III clinical trials, **Ensitrelvir** also demonstrated rapid clearance of the infectious SARS-CoV-2 virus, with the percentage of patients with positive virus titers on day 4 of treatment (after the third dose) reduced by approximately 90% compared to placebo; compared to placebo, **Ensitrelvir** reduced the duration of shedding of SARS-CoV-2 by 1−2 days. More importantly, five key COVID-19 symptoms of SARS-CoV-2 omicron variant infection (nasal congestion or sore throat, runny nose, cough, low energy or fatigue, fever or body temperature) were relieved for the first time after the patient took **Ensitrelvir**.[41,120]

WU-04 (**WPV01**)[46] is an orally administered, noncovalent inhibitor that is a potent inhibitor of SARS-CoV-2 by research at Westlake University (Figure 9B). The investigators evaluated the antiviral activity of the inhibitor in A549-hACE2 cells, which showed good inhibition with an EC_{50} of 12 nM. Meanwhile, it also showed efficient inhibitory activity in NHBE and Vero E6 cells (EC_{50} of 3 and 10 nM, respectively). Moreover, **WU-04** showed excellent inhibition effects in various variants of SARS-CoV-2. In Caco-2 and A549-TMPRSS2-ACE2 cells, the EC_{50} values of the inhibitor acting on the Delta variant were 21 and 10 nM, respectively. **WU-04** showed a better EC_{50} of 24 nM against the Omicron variant in Caco-2 cells compared to PF-07321332 (EC_{50} = 33 nM). At the same time, **WU-04** exhibited antiviral activity similar to that of Nirmatrelvir in K2-hACE07321332 mice under the same conditions of oral dosing. The crystal structure shows that the nitrogen atom and the carbonyl group attached to it on the isoquinoline ring of **WU-04** form hydrogen bonds with His163 and Asn142, respectively. Its pharmacokinetics showed that WU-04 exhibited antiviral activity similar to that of Nirmatrelvir in K2-hACE07321332 mice under the same conditions of oral dosing. It formed a hydrogen bond between the carbonyl oxygen of the methylcarbamoyl group and the Glu166 backbone amide. At the same time, the nitro group has a powerful electron-withdrawing capacity, which further

https://doi.org/10.1021/acsomega.4c03023
ACS Omega 2024, 9, 34196−34219

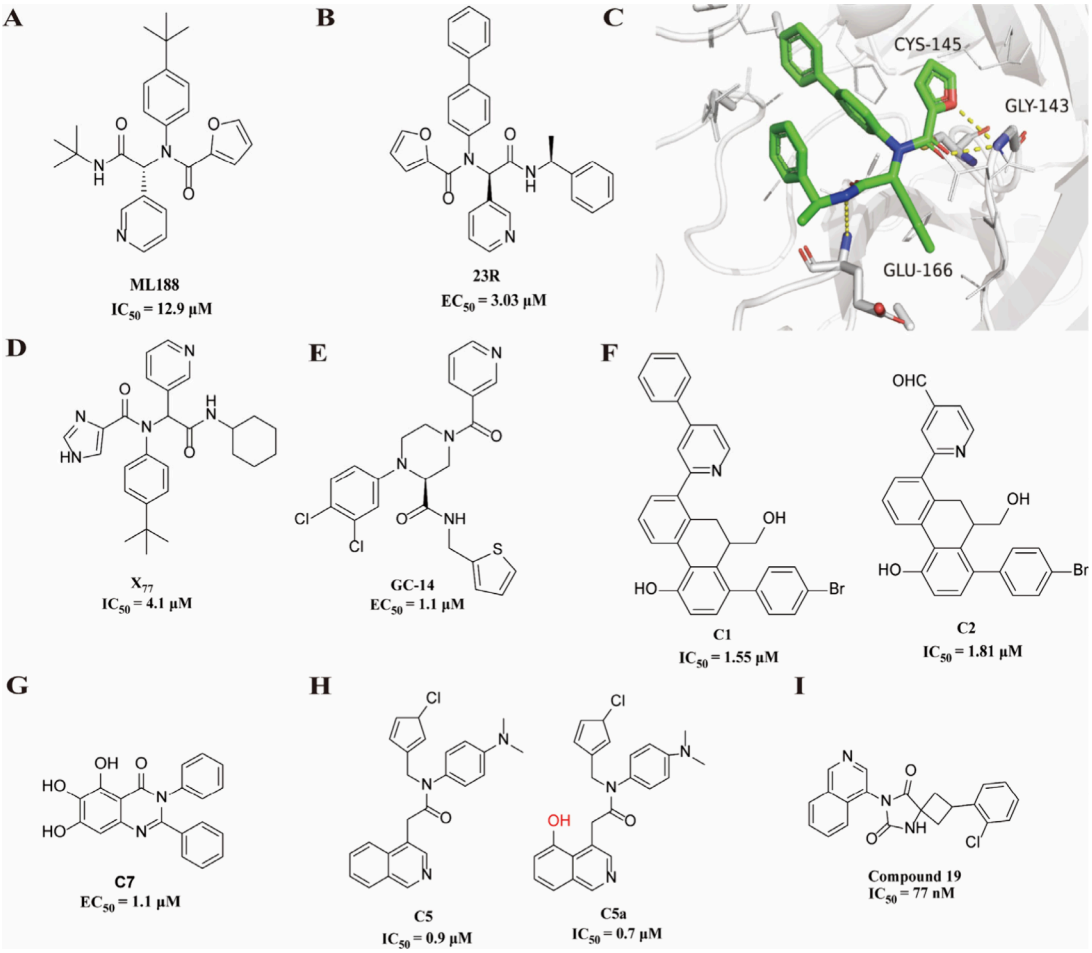

Figure 10. Molecular structure of **ML188** (A). The molecular structure (B) and crystal structure (C) of **23R** (PBD: 7KX5). The molecular structure of **X77** (D), **GC-14** (E), **C1**, **C2** (F), **C7** (G), **C5** and **C5a** (H) (differences between the two molecules are marked in red), and **Compound 19** (I).

enhances interactions of the halogen bond between the Thr190 carbonyl group and the bromide. In conclusion, **WU-04** showed excellent results in terms of both antiviral action and oral efficacy. Currently, WU-04[47] is in the clinical phase III.

Masitinib (Figure 9C) is an oral c-Kit inhibitor currently in phase II and III cancer clinical studies. **Masitinib** was also studied to exhibit significant inhibitory activity against SARS-CoV-2-M^{pro} (IC_{50} = 2.5 μM).[51] Studies at the cellular level have shown that the incorporation of **Masitinib** 2 h after SARS-CoV-2 infection effectively inhibits the replication of SARS-CoV-2 wild-type and several major prevalent variants of the virus. The crystal structure shows that **Masitinib** binds noncovalently to M^{pro} structural domains I and II and inhibits the key active site residues of the dimer, with the pyridine nucleus binding to the S1M^{pro} peptide-recognizing site and the toluene nucleus forming a stable $\pi-\pi$ conjugation effect with the S2 pocket (Figure 9H). In a randomized, double-blind, placebo-controlled Phase II clinical trial, **Masitinib** demonstrated antiviral activity in symptomatic people with mild to moderately severe COVID-19.

Frank von Delft's group[121] successfully introduced a tetrahydropyran ring into the P2 pocket of the SARS-CoV-2 main protease, effectively converting the P2 substituent into a chromane moiety. The compound, designated as **MAT-POS-b3e365b9-1**, was initially synthesized with an IC_{50} value of 360 nM for the racemic mixture **VLA-UCB-1dbca3b4-15**. In their subsequent investigations, the researchers further explored the P2 pocket by replacing tetrahydroisoquinoline with chromanes. They introduced a functionalized handle, **MAT-POS-3ccb8ef6-1**, and constructed a focused library through sulfonamide Schotten Baumann coupling. A comprehensive evaluation of the antiviral activity, absorption, distribution, metabolism, excretion (ADME), and pharmacokinetic (PK) properties of compound **MAT-POS-e194df51-1** was conducted (Figure 9D). Notably, the EC_{50} of **MAT-POS-e194df51-1** was determined to be 64 nM in A549-ACE2-TMPRSS2 cells and 126 nM in HeLa-ACE2 cells. Moreover, this lead compound exhibited good cross-reactivity against known SARS-CoV-2 variants, including Alpha, Beta, Delta, and Omicron, demonstrating its potential as a favorable therapeutic candidate.

Yu's team[122] investigated a dual-target (M^{pro} and PL^{pro}) covalent inhibitor, **LY1** (Figure 9E). Among other things, due to the specificity of **LY1**, the investigators tested its k_{inact}/K_i values (M^{pro} with k_{inact}/K_i values of 710 M^{-1} S^{-1} and PL^{pro} with k_{inact}/K_i values of 500 M^{-1} s^{-1}). Next, the researchers verified the selectivity of **LY1** for two cysteine proteases and a group of serine proteases. Their results showed that the inhibitors exhibited significant inhibitory activity against the two cysteine proteases and essentially had no inhibitory activity against the serine proteases tested. Thus, **LY1** has some

https://doi.org/10.1021/acsomega.4c03023
ACS Omega 2024, 9, 34196−34219

high selectivity. The crystal structures of the open form of **LY1** (**LY1-O**) and SARS-CoV-2-M^{pro} show that the inhibitor forms $\pi-\pi$ stacking with His41 and hydrogen bonding with Gly143, respectively, thus further strengthening their interaction. In the S1′ and S2 sites, the sulfonamide group of **LY1** forms hydrogen bonds with Thr25 and Cys44, respectively. At the S1 site, the amino group of the piperazine ring of **LY1-O** forms hydrogen bonds with His164 and Asn142, respectively (Figure 9F). While **LY1** demonstrates modest activity, its structural analysis offers promising opportunities for optimization. Particularly, the potential exists to enhance its inhibitory potency through modifications at the S1 and S4 sites. This positions **LY1** as a strong foundation for future inhibitor research, paving the way for the development of more effective inhibitors against M^{pro} and PL^{pro}.

ML188 (Figure 10A) emerged from high-throughput screening as a potent noncovalent inhibitor of SARS-CoV M^{pro}, demonstrating notable antiviral activity in SARS-CoV Urbani-infected Vero E6 cells (EC_{50} = 12.9 μM). The crystal structure shows that the pyridine at the S1 site in **ML188** can form hydrogen bonds with the imidazole His163 in the side chain and that both the furan oxygen and its amide oxygen can form hydrogen bonds with the amide Gys143 in the main chain, enabling ML188 to achieve stable binding to M^{pro}.[123] The Lockblum group[124] found that ML188 has a better affinity for SARS-CoV-2-M^{pro} than SARS-CoV-M^{pro}. Based on the **ML188** structure, **23R** (Figure 10B), designed and synthesized by Naoya's group,[125] showed significant inhibitory activity against SARS-CoV-2-M^{pro} with an IC_{50} value of 0.20 μM. It was effective in inhibiting the replication of SARS-CoV-2 in Calu-3 cells (EC_{50} = 3.03 μM) and was noncytotoxic at 100 μM. The furan-based portion of **23R** binds to a portion of the P1′ site, which normally accommodates small hydrophobic residues. Although the furan amide carbonyl of **23R** does not insert into the oxygen anion cavity, it forms a divergent hydrogen bond with the apical residue Gly143 of this oxygen anion cavity. The amide bond connecting the pyridine ring and the α-methylbenzyl moiety forms a hydrogen bond with the backbone of Glu166. The benzyl ring moiety of the α-methyl benzyl moiety is in the S2 and S4 pockets, a novel binding pose that has not been observed in existing M^{pro} inhibitors (Figure 10C). In particular, the binding site of **23R** has continuous intramolecular π-stacking in which the phenyl group is sandwiched between the furan and benzyl groups, which may contribute to its effective inhibition of M^{pro}.

Andrianov et al.[126] used a computer to design a noncovalent compound **X77** with a high affinity for SARS-CoV-2-M^{pro} (Figure 10D). Using a combination of molecular docking, quantum chemical calculations, and MD simulations, the researchers showed that **X77** has a high affinity for the catalytic site of SARS-CoV-2-M^{pro}. Thus, **X77** mimetic drug candidates could be used as a novel backbone for designing pockets of activity targeting SARS-CoV-2-M^{pro}.

GC-14 (Figure 10E) is a noncovalent inhibitor designed based on MCULE-5948770040.[127] The crystal structure of **GC-14** with M^{pro} shows[128] that the newly introduced nicotinic acid moiety perfectly occupies the S1 pocket and binds to the imidazole NH of His163 via hydrogen bonding, and this optimization enhances the antiviral action of the compound. Experiments in Vero E6 cells have shown that **GC-14** has some antiviral effects (EC_{50} = 1.1 μM) and did not exhibit cytotoxicity (CC_{50} > 100 μM). At the same time, its specificity for M^{pro} makes it much less risky to produce side effects in a treatment. Unfortunately, its oral availability is low. Therefore, further enhancement of studies on the oral availability of **GC-14** will help to facilitate research on oral inhibitors of SARS-COV-2.

The 9,10-dihydrophenanthrene derivative[129] is a noncovalent inhibitor of SARS-CoV-2-M^{pro}. The investigators screened the internal compound library using FRET (fluorescence resonance energy transfer) and found the best inhibitory activity for **C1** and **C2** (Figure 10F) (IC_{50} values of 1.55 and 1.81 μM, respectively; K_i values of 6.09 and 7.64 μM, respectively). Molecular docking studies showed that an essential reason for its inhibitory SARS-CoV-2-M^{pro} activity was the hydrogen bond formation between the phenolic hydroxyl group of **C1** and the critical residue Glu290 at the dimer interface. Meanwhile, hydrophobic interactions with Phe3 and Tyr126 residues increase the affinity of **C1** for M^{pro}. For the substrate binding pocket, the 4-bromophenyl moiety is inserted deeply into the S2 site of M^{pro}, which is large enough to accommodate large hydrophobic fragments. In addition, compound **C1** showed excellent metabolic stability in the human gastrointestinal tract, plasma, and liver microsomes. It, therefore, has high potential as a new oral drug.

Xiangyu Zhang's research group[130] has identified a series of SARS-CoV-2 M^{pro} inhibitors based on quinazolin-4-one by modifying the core chromium-4-one of baicalein into quinazolin-4-one (initially employing a scaffold hopping strategy). Among these inhibitors, compound **C7** (Figure 10G) demonstrated excellent target specificity. In vitro DMPK analysis revealed that **C7** exhibited high metabolic stability in human liver microsomes when it was incubated with NADPH alone as a cofactor. The FRET enzyme assay demonstrated significant inhibitory activity of **C7** against various human proteases (IC_{50} > 10 μM), while the CCK-8 assay indicated low cytotoxicity of **C7** toward Vero E6 cells (CC_{50} > 50 μM) and an EC_{50} value of 1.10 μM in Vero E6 cells infected with SARS-CoV-2. Notably, **C7** displayed superior M^{pro} inhibitory potency and antiviral activity compared to baicalein, making it a promising lead compound for further development as an M^{pro} inhibitor.

François Jean's team[131] used free energy perturbation (FEP) simulations to design and synthesize a series of **C1**−**C5** compounds, with **C5** and **C5a** showing better activity and high synthetic treatability (Figure 10H). **C5** and **C5a** were found to be potent inhibitors of the hydrolytic activity of SARS-CoV-2 -M^{pro} endoproteins in cellulose as assessed by a live cell assay with IC_{50}'s of 70 and 30 nM, respectively. The researchers then tested it in Calu-3 and caco-2 cells, and **C5** had EC_{50}'s of 0.2−0.7 and 0.1−0.3 μM when stained with dsDNA and nucleocapsid, respectively. The EC_{50} of **C5a**, on the other hand, was 28−95 nM and 30−69 nM, suggesting that both showed better inhibition of SARS-CoV-2 Omicron BA.5, BQ.1.1, and XBB.1.5 in Calu-3 and caco-2 cell lines. During dosing for the treatment of SARS-CoV-2 Omicron BA.5, **C5a** can synergize with N-0385 or bafilomycin D. It is believed that the oral efficacy of the drug will be more significant after improving pharmacokinetic and safety issues.

Jens Carlsson's team[132] developed a noncovalent host protein inhibitor, **Compound 19** (Figure 10I), by optimizing lead compounds and incorporating optimal substituents at the S1 and S2 sites. The compound exhibited increased potency and affinity with the introduction of a phenyl ring with an *o*-chloro substituent in the aliphatic tail, using pyridinyl-hydantoin as a scaffold (IC_{50} = 0.077 μM, K_d = 0.038 μM).

https://doi.org/10.1021/acsomega.4c03023
ACS Omega 2024, 9, 34196−34219

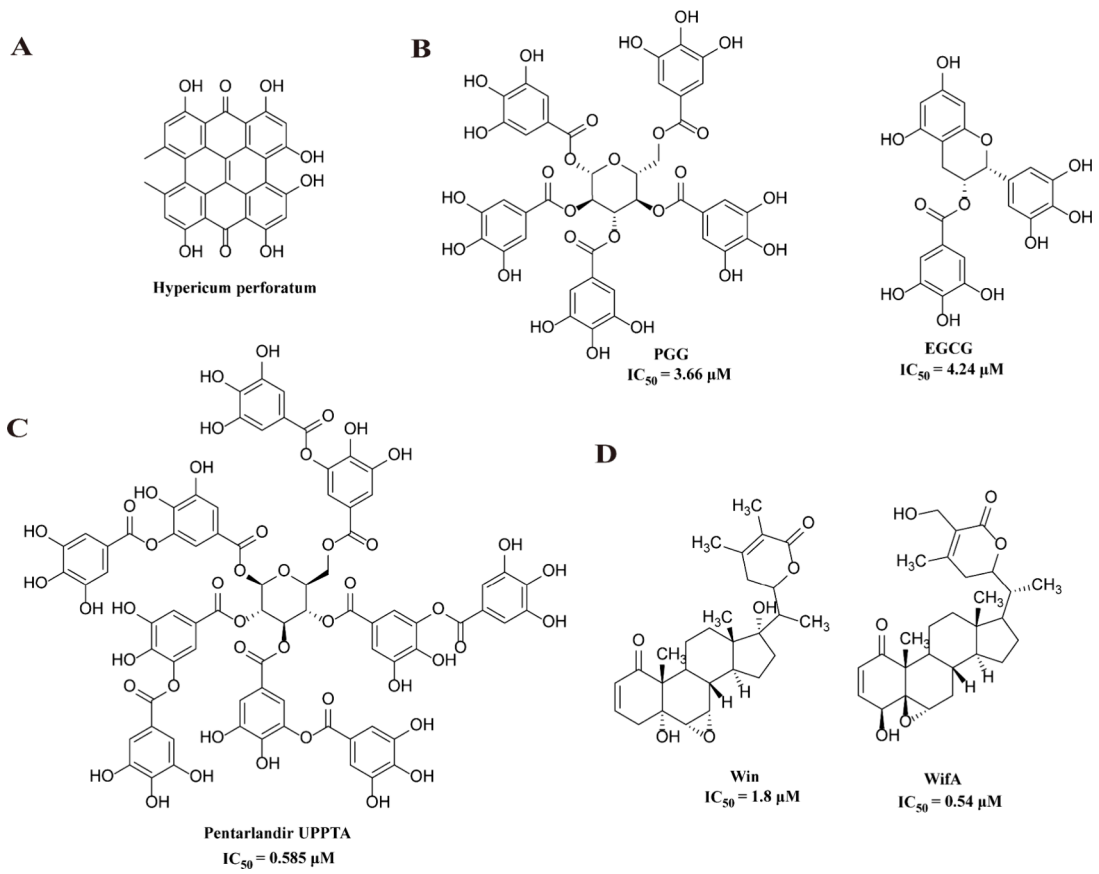

Figure 11. Molecular structure of **Hypericum perforatum** (A), **PGG** and **EGCG** (B), **Pentarlandir UPPTA** (C), and **Win** and **WifA** (D).

Cell-based assays and in vitro pharmacokinetic analyses demonstrated that **Compound 19** effectively inhibited SARS-CoV-1 (EC_{50} = 0.39 μM, Vero E6 cells) and MERS-CoV (EC_{50} = 0.20 μM, Huh7 cells) while maintaining good metabolic stability.

The principal distinction between covalent and noncovalent inhibitors is that covalent inhibitors irreversibly "switch off" the target protein by forming a covalent bond with the target protein. This results in a longer binding time with the target protein and stronger binding ability, which can effectively reduce the number of times the patient takes the drug and lower the required effective concentration. However, covalent inhibitors carry the risk of unpredictable toxicity or irreversible damage. On the contrary, noncovalent inhibitors engage with the target protein through reversible interactions such as hydrogen bonds, ionic interactions, and hydrophobic interactions. These weaker interactions may help minimize potential side effects and off-target effects.[133,134]

3.3. Natural Product Inhibitors. **Hypericum perforatum** (Figure 11A) is a widely distributed herbal plant with anti-inflammatory and antibacterial properties.[135] Researchers[136] obtained quantitative dried extracts (HP1) of the flowering place of *Aconitum perforatum* by methanol−water extraction, drying, and treatment of the flowering place of **Hypericum perforatum**, the main component of which is hypericin. Subsequent antiviral testing of Vero cells by the investigators found that 25 ng/mL chrysin completely blocked the multiplication of early SARS-CoV-2. Hypericin also had the same viral inhibitory effect on SARS-CoV-2 variants B.1.351, B.1.1.7, and B.1.617.2. In vitro studies showed that only hypericin treatment of cells after SARS-CoV-2 infection reduced viral load significantly. This suggests that hypericin may have a direct antiviral activity against SARS-CoV-2 particles in newly produced or secreted supernatants.

PGG and **EGCG** are a class of natural inhibitors with developmental value in a variety of diseases[137−140] (Figure 11B). Huang's group tested the inhibition of SARS-CoV-2-M^{pro} by **PGG** and **EGCG** in different concentrations of the protease with the help of FRET, and their IC_{50} values were 3.66 and 4.24 μM, which showed their potential in the inhibition of SARS-CoV-2.[141] On this basis, the Shi team[50] developed a new inhibitor, **Pentarlandir UPPTA**, whose active pharmaceutical ingredient (API) is tannic acid with varying amounts of galloyl moieties, which have antioxidant properties (Figure 11C). It can effectively inhibit the replication of SARS-CoV-2, and it has an EC_{50} of 0.585 μM in Vero E6 cells. In lung experiments, oral **Pentarlandir UPPTA** did not adversely affect the lungs when it reached its highest concentration in the lungs. Toxicological studies have shown that this inhibitor is safe and has no significant adverse effects at doses of up to 2000 mg/kg in rats. **Pentarlandir UPPTA** is currently in clinical phase II (NCT04911777) and requires further exploration of its safety and pharmacological efficacy in humans.

Withania somnifera is an important medicinal plant in mainland India.[142] Goutam Chowdhury's group[143] obtained two natural products **withaferin A** (**wifA**) and **withanone** (**win**) from the herb using docking studies and CMap analysis (Figure 11D). The activity assay showed that **wifA** and **win** had good activity with IC_{50} values of 0.54 and 1.8 μM, respectively. The study of both structures shows that both **wifA** and **win** have the potential to bind and form covalent

https://doi.org/10.1021/acsomega.4c03023
ACS Omega 2024, 9, 34196−34219

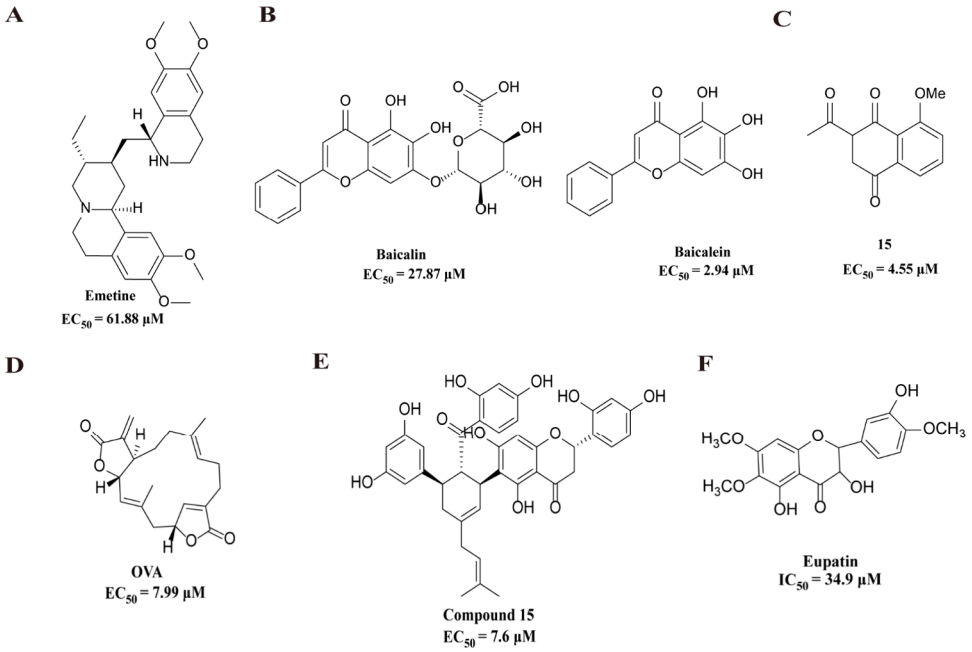

Figure 12. Molecular structure of **Emetine** (A), **Baicalin** and **Baicalin** (B), **Compound 15** (C), **OVA** (D), **Compound 15** (E), and **Eupatin** (F).

complexes with Cys145 thiols of M^{pro} and increase stability by binding to Cysteine (Cys) and Glutathione (GSH).

Emetine, a tetrahydroisoquinoline alkaloid, consists of five loops and exhibits potent inhibitory effects on various coronaviruses without inducing drug resistance.[144] Research by Yan's team revealed that Emetine effectively suppressed SARS-CoV-2 replication in Vero E6 cells, with an EC_{50} value of 0.46 μM[145,146] (Figure 12A). However, Valipour's team showed that while the drug displayed antiviral activity against SARS-CoV-2 it also caused heart-related side effects, leading to significant restrictions in its clinical application.

Baicalin and **Baicalein** (Figure 12B) were applied to the study of SARS-CoV-2 M^{pro} inhibitors.[147−149] Xu's team found that both exhibited a dose-dependent inhibition of SARS-CoV-2 replication in VeroE6 cells with EC_{50} values of 27.87 and 2.94 μM, respectively.[150] However, investigators have not published insights into **Baicalin** and **Baicalein** in clinical trials in animal models or as clinical agents for COVID-19 patients. Meanwhile, methods to improve its oral bioavailability as an anti-SARS-CoV-2 and anti-inflammatory agent remain deficient. Therefore, the possibility of using it as a lead compound in the future needs to be further evaluated.[151]

Rao's team[97] utilized FRET to screen for the natural naphthoquinone shikonin, which was found to be toxic. Subsequently, Cui's team[152] employed a skeleton simplification strategy to optimize it, resulting in the synthesis of 2-acetyl-8-methoxy-1,4-naphthoquinone (**Compound 15**) (Figure 12C). The cytotoxicity of **Compound 15** was evaluated on human normal fibroblast HFF-1 cells using a standard MTT assay, revealing lower toxicity with an IC_{50} of 41.2 μM. In vitro antiviral activity assessment demonstrated some antiviral potential with an EC_{50} of 4.55 μM. Crystal structure analysis revealed that **Compound 15** exhibited strong binding and interaction with M^{pro}, suggesting its potential as an M^{pro} activity inhibitor.

Huang's group[153] conducted an in-depth study on the pharmacological mechanism of the macrocyclic diterpenoid ovalbumin (**OVA**) in inhibiting SARS-CoV-2 infection and pulmonary fibrosis in vitro and in vivo (Figure 12D). The study finds that **OVA** significantly impeded the proteolysis activity of SARS-CoV-2-M^{pro} by interacting stably with three core pharmacophore anchors and the catalytic dyad (H41 and C145) of SARS-CoV-2-M^{pro}. Evaluation of Vero E6 cells showed that when treated with **OVA** alone it reduced SARS-CoV-2 infection in a dose-dependent manner (EC_{50} = 7.9 μM), with 15 μM **OVA** reducing viral infection by more than 90%. In contrast, synergistic inhibition was produced when 10 μM of the OVA was combined with 1 μM of the REM (CI = 0.767 μM), which was more inhibitory than **OVA** alone. When **OVA** was administered to mice with BLM-induced pulmonary fibrosis, it improved inflammatory cell infiltration and collagen deposition in the lungs of mice and reduced the levels of profibrotic and proinflammatory biomarkers in mice. However, the therapeutic effect of **OVA** in patients with COVID-19 pulmonary fibrosis needs to be further elucidated.

Judith M. Rollinger's team[154] found that mulberry Diels−Alder-type adducts (MDAAs) are a novel class of M^{pro} inhibitors and have strong anti-SARS-CoV-2 activity through screening of natural product databases. First, the investigators used 5-FAM-AVLQSGFR-Lys (Dabcyl)-K-amide as a substrate in 20 and 100 μM of SARS-CoV-2-M^{pro} to detect the protease activities of the virtually predicted 19 M^{pro} VHs (11−29) using a fluorescence resonance energy transfer quenching method. Among them, 12−16 showed a better inhibitory effect with IC_{50} values of 7.24, 6.70, 13.85, 4.82, and 5.25 μM, respectively. After that, the researchers tested their antiviral activity against SARS-CoV-2 in Calu-3 cells, and **Compounds 12**, **13**, and **15** (Figure 12E) significantly inhibited the replication of SARS-CoV-2 with IC_{50} values of 4.6, 8.0, and 7.6 μM. The three were cytotoxic at higher concentrations, even so they showed good selectivity against SARS-CoV-2 with SIs of 5.1, 3.1, and 6.5, respectively, and the three showed excellent binding ability in molecular docking analyses as well as NMR experiments. Meanwhile, MDAA has been shown to possess certain anti-infective and anti-inflammatory characteristics in previous studies.[155] Therefore, it is expected to be a new drug

https://doi.org/10.1021/acsomega.4c03023
ACS Omega 2024, 9, 34196−34219

for the treatment of COVID-19 but still needs further clinical evaluation.[156]

Junsoo Park and colleagues[157] isolated **Eupatin** from *Inula japonica* flowers and showed that this compound inhibited SARS-CoV-2-M^{pro} as well as SARS-CoV-2 replication (Figure 12F). First, the researchers chromatographically separated the extract and identified it as **Eupatin**, and second, using enzyme kinetic analysis, they showed that the compound could bind stably to the M^{pro} active site. Molecular dynamics studies showed that the two could move stably and fluidly. The effect of **Eupatin** on coronavirus replication was subsequently assessed with the aid of a plaque formation assay. The results of RD cells treated with mock or **Eupatin** and infected with HCoV-OC43 showed that high concentrations of **Eupatin** ($\geq$10 μM) resulted in cytotoxicity, whereas lower concentrations (0.5−5 μM) significantly inhibited coronavirus replication. Unfortunately, due to strict regulations, SARS-CoV-2 was not used in this experiment, and HCoV-OC43, which belongs to the same β-coronavirus family, was chosen instead.

Furthermore, the researchers used in silico and in vitro methods to investigate the potential efficacy of cranberry fruit in the treatment of COVID-19. Cyanidin epicatechin, β-carotene, and 3-*O*-galactoside were found to be the three most prominent compounds in cranberry that showed robust interactions with the M^{pro} through molecular docking and molecular dynamic simulation analyses.[158] Meanwhile, Jin's team discovered natural products obtained from Traditional Chinese Medicine (TCM) that could also be useful for anti-COVID-19 research. Active compounds in TCM have similarly demonstrated the advantages of their action with M^{pro} through noncovalent interactions with critical amino acids (e.g., HIS 41, ASN 142, GLY 143, MET 165, GLU 166, or GLN 189) by occupying different subsites (S1, S2, S3, and S4) of the SARS-CoV-2 M^{pro} active site in a specific stance.[159]

These findings illustrate the diverse array of natural compounds being investigated for their antiviral properties against SARS-CoV-2, each offering unique mechanisms of action and therapeutic potentials. The exploration of these natural inhibitors continues to provide valuable insights into the development of effective treatments for COVID-19.

4. CONCLUSIONS AND OUTLOOK

Throughout the COVID-19 pandemic, significant strides have been made in vaccine development, leading to several vaccines being widely administered. Despite these advancements, the high mutation and recombination rates of SARS-CoV-2 present ongoing challenges as the virus evolves at a pace that can outstrip vaccine development efforts. As a result, there is a pressing need to create anti-COVID-19 drugs to address both present and future outbreaks. Small-molecule oral drugs are particularly advantageous in this regard.

The SARS-CoV-2 M^{pro} has emerged as a significant target for the development of novel broad-spectrum antiviral drugs due to its high conservation throughout evolution. So far, hundreds of crystal structures of SARS-CoV-2 M^{pro} have been reported, which have greatly accelerated the development of SARS-CoV-2 M^{pro} inhibitors. Of these, most of the potent inhibitors are peptidomimetic compounds with electrophilic "warheads" that covalently bind to Cys145, and researchers have designed more potent inhibitors based on the characteristics of each warhead. For example, although the nitrile-containing warhead is less reactive, it usually has excellent target specificity and metabolic stability. Nonpeptidomimetic compounds tend to resist enzyme-mediated hydrolysis and can improve pharmacokinetics. In addition, noncovalent inhibitors can bind to target proteins through reversible interactions and may help minimize potential side effects and off-target effects. However, the limitations inherent in some of the nonspecific classes of drugs have seriously hampered the research of inhibitors, such as **Ebselen**'s multitargeting action of toxic side effects, which makes it greatly limited for clinical use. The emergence and widespread application of many specific inhibitors not only has provided significant support for the control of the current outbreak but also has the potential to open new directions for future research on novel inhibitors. For example, **nirmatrelvir** reduces the risk of hospitalization or death by 89% in patients with novel coronary venous pneumonia, as well as has the advantages of being less likely to be resistant to the drug and being effective against mutant strains, which makes it considered the golden inhibitor.

However, the virus's high mutation rate poses a challenge to current drug development endeavors; thus, multitarget antiviral inhibitors can more effectively overcome drug resistance. At present, some of the existing marketed drugs have a high degree of scaffold similarity; therefore, researchers are advised to explore the use of AI technology or seek out more potent compounds with entirely new scaffolds derived from natural sources, thus enriching the diversity of drug classes. Numerous promising inhibitors are still in the preclinical stages, highlighting the need for additional clinical validation. Natural products are essential in identifying potential SARS-CoV-2 M^{pro} drug candidates. First, most natural products are primarily assessed at the molecular and cellular levels, lacking evaluation at the animal level, a crucial step toward clinical drug development. Second, challenges persist in the total synthesis of natural products. Discovering superior lead compounds and effectively optimizing them are key challenges in drug research and development. In addition to the above, other effective strategies, such as cyclic peptides, dual-targeted drugs, proteolysis targeting chimera (PROTAC), and combined treatment, have great potential. Among them, PROTAC is an advanced technology in precision medicine that enables targeted protein degradation. There is significant potential in utilizing PROTAC-mediated protein degradation to develop antivirals targeting M^{pro}, which could be effective against drug-resistant viral variants.

In the future, we believe that with continuous technological advancement and research progress, novel and efficient small-molecule inhibitors can be used for the treatment of novel coronavirus infections. At the same time, we also need to strengthen international cooperation to jointly respond to the spread of viruses and epidemics and to make greater contributions to the maintenance of global public health security.

AUTHOR INFORMATION

Corresponding Author

Xiao-Long Liu − *School of Medicine, Yan'an University, Yan'an 716000, China*; Email: lxl3281@163.com

Authors

Yue Yang − *School of Medicine, Yan'an University, Yan'an 716000, China*

Yi-Dan Luo − *School of Medicine, Yan'an University, Yan'an 716000, China*; orcid.org/0009-0001-2811-032X

https://doi.org/10.1021/acsomega.4c03023
ACS Omega 2024, 9, 34196−34219

Chen-Bo Zhang − *School of Medicine, Yan'an University, Yan'an 716000, China*
Yang Xiang − *School of Medicine and College of Physical Education, Yan'an University, Yan'an 716000, China*
Xin-Yue Bai − *School of Medicine, Yan'an University, Yan'an 716000, China*
Die Zhang − *School of Medicine, Yan'an University, Yan'an 716000, China*
Zhao-Ying Fu − *School of Medicine, Yan'an University, Yan'an 716000, China*
Ruo-Bing Hao − *School of Medicine, Yan'an University, Yan'an 716000, China*

Complete contact information is available at: https://pubs.acs.org/10.1021/acsomega.4c03023

Author Contributions

#Y.Y., Y.-D.L., C.-B.Z., and Y.X. share the first authorship. Yue Yang, Yi-Dan Luo, Chen-Bo Zhang, and Yang Xiang are the cofirst authors of this paper and were responsible for writing and revising the text. Xin-Yue Bai and Die-Zhang are the second authors responsible for the data collection. Zhao-Ying Fu and Ruo-Bin Hao are the third authors responsible for the revision. Xiao-Long Liu is the corresponding author responsible for the conceptualization and financial support, guidance, and responsibility for the article. All authors have read and approved the final manuscript.

Funding

This study was supported by the Natural Science Foundation of Yan'an University, the Shaanxi Provincial Health Research Fund, the Natural Science Foundation of Shaanxi Province and the Shaanxi Provincial Department of Education Research Project (YDBK2020-28, 2022E010, 2023-JC-QN-0125, and 22JK0612 to L.X.L.), and the Key Research and Development Project of Shaanxi Province (2022SF-393 to F.Z.Y.).

Notes

The authors declare no competing financial interest.

REFERENCES

(1) Gorbalenya, A. E. The species Severe acute respiratory syndrome-related coronavirus: classifying 2019-nCoV and naming it SARS-CoV-2. *Nature microbiology* **2020**, *5* (4), 536−544.
(2) Zou, L.; Ruan, F.; Huang, M.; Liang, L.; Huang, H.; Hong, Z.; Yu, J.; Kang, M.; Song, Y.; Xia, J.; Guo, Q.; Song, T.; He, J.; Yen, H. L.; Peiris, M.; Wu, J. SARS-CoV-2 Viral Load in Upper Respiratory Specimens of Infected Patients. *N Engl J. Med.* **2020**, *382* (12), 1177−1179.
(3) Lu, N.; Gu, T.; Tian, X.; Zhao, S.; Jin, G.; Mangaladoss, F.; Qiao, Y.; Liu, K.; Zhao, R.; Dong, Z. Acetylshikonin inhibits inflammatory responses and Papain-like protease activity in murine model of COVID-19. *Signal transduction and targeted therapy* **2022**, *7* (1), 371.
(4) Wang, Q.; Iketani, S.; Li, Z.; Liu, L.; Guo, Y.; Huang, Y.; Bowen, A. D.; Liu, M.; Wang, M.; Yu, J.; Valdez, R.; Lauring, A. S.; Sheng, Z.; Wang, H. H.; Gordon, A.; Liu, L.; Ho, D. D. Alarming antibody evasion properties of rising SARS-CoV-2 BQ and XBB subvariants. *Cell* **2023**, *186* (2), 279−286.
(5) Carabelli, A. M.; Peacock, T. P.; Thorne, L. G.; Harvey, W. T.; Hughes, J.; de Silva, T. I.; Peacock, S. J.; Barclay, W. S.; de Silva, T. I.; Towers, G. J.; Robertson, D. L. SARS-CoV-2 variant biology: immune escape, transmission and fitness. *Nat. Rev. Microbiol* **2023**, *21* (3), 162−177.
(6) Markov, P. V.; Ghafari, M.; Beer, M.; Lythgoe, K.; Simmonds, P.; Stilianakis, N. I.; Katzourakis, A. The evolution of SARS-CoV-2. *Nat. Rev. Microbiol* **2023**, *21* (6), 361−379.
(7) Uriu, K.; Ito, J.; Zahradnik, J.; Fujita, S.; Kosugi, Y.; Schreiber, G.; Sato, K. Enhanced transmissibility, infectivity, and immune resistance of the SARS-CoV-2 omicron XBB.1.5 variant. *Lancet Infect Dis* **2023**, *23* (3), 280−281.
(8) Wang, Z.; Yang, L. Post-acute Sequelae of SARS-CoV-2 Infection: A Neglected Public Health Issue. *Front Public Health* **2022**, *10*, 908757.
(9) Davis, H. E.; McCorkell, L.; Vogel, J. M.; Topol, E. J. Long COVID: major findings, mechanisms and recommendations. *Nat. Rev. Microbiol* **2023**, *21* (3), 133−146.
(10) Blomberg, B.; Mohn, K. G.; Brokstad, K. A.; Zhou, F.; Linchausen, D. W.; Hansen, B. A.; Lartey, S.; Onyango, T. B.; Kuwelker, K.; Sævik, M.; Bartsch, H.; Tondel, C.; Kittang, B. R.; Cox, R. J.; Langeland, N.; et al. Long COVID in a prospective cohort of home-isolated patients. *Nat. Med.* **2021**, *27* (9), 1607−1613.
(11) Cheng, V. C.; Lau, S. K.; Woo, P. C.; Yuen, K. Y. Severe acute respiratory syndrome coronavirus as an agent of emerging and reemerging infection. *Clin Microbiol Rev.* **2007**, *20* (4), 660−94.
(12) Shehzadi, K.; Saba, A.; Yu, M.; Liang, J. Structure-Based Drug Design of RdRp Inhibitors against SARS-CoV-2. *Top Curr. Chem. (Cham)* **2023**, *381* (5), 22.
(13) Park, G. J.; Osinski, A.; Hernandez, G.; Eitson, J. L.; Majumdar, A.; Tonelli, M.; Henzler-Wildman, K.; Pawłowski, K.; Chen, Z.; Li, Y.; Schoggins, J. W.; Tagliabracci, V. S. The mechanism of RNA capping by SARS-CoV-2. *Nature* **2022**, *609* (7928), 793−800.
(14) Malone, B.; Urakova, N.; Snijder, E. J.; Campbell, E. A. Structures and functions of coronavirus replication-transcription complexes and their relevance for SARS-CoV-2 drug design. *Nat. Rev. Mol. Cell Biol.* **2022**, *23* (1), 21−39.
(15) Chan, J. F.; Lau, S. K.; To, K. K.; Cheng, V. C.; Woo, P. C.; Yuen, K. Y. Middle East respiratory syndrome coronavirus: another zoonotic betacoronavirus causing SARS-like disease. *Clin Microbiol Rev.* **2015**, *28* (2), 465−522.
(16) Li, G.; De Clercq, E. Therapeutic options for the 2019 novel coronavirus (2019-nCoV). *Nat. Rev. Drug Discov* **2020**, *19* (3), 149−150.
(17) V'Kovski, P.; Kratzel, A.; Steiner, S.; Stalder, H.; Thiel, V. Coronavirus biology and replication: implications for SARS-CoV-2. *Nat. Rev. Microbiol* **2021**, *19* (3), 155−170.
(18) Yang, H.; Rao, Z. Structural biology of SARS-CoV-2 and implications for therapeutic development. *Nat. Rev. Microbiol* **2021**, *19* (11), 685−700.
(19) Walker, A. P.; Fan, H.; Keown, J. R.; Knight, M. L.; Grimes, J. M.; Fodor, E. The SARS-CoV-2 RNA polymerase is a viral RNA capping enzyme. *Nucleic Acids Res.* **2021**, *49* (22), 13019−13030.
(20) Yin, W.; Mao, C.; Luan, X.; Shen, D. D.; Shen, Q.; Su, H.; Wang, X.; Zhou, F.; Zhao, W.; Gao, M.; Chang, S.; Xie, Y. C.; Tian, G.; Jiang, H. W.; Tao, S. C.; Shen, J.; Jiang, Y.; Jiang, H.; Xu, Y.; Zhang, S.; Zhang, Y.; Xu, H. E. Structural basis for inhibition of the RNA-dependent RNA polymerase from SARS-CoV-2 by remdesivir. *Science* **2020**, *368* (6498), 1499−1504.
(21) Poduri, R.; Joshi, G.; Jagadeesh, G. Drugs targeting various stages of the SARS-CoV-2 life cycle: Exploring promising drugs for the treatment of Covid-19. *Cell Signal* **2020**, *74*, 109721.
(22) Arya, R.; Kumari, S.; Pandey, B.; Mistry, H.; Bihani, S. C.; Das, A.; Prashar, V.; Gupta, G. D.; Panicker, L.; Kumar, M. Structural insights into SARS-CoV-2 proteins. *J. Mol. Biol.* **2021**, *433* (2), 166725.
(23) Anand, K.; Ziebuhr, J.; Wadhwani, P.; Mesters, J. R.; Hilgenfeld, R. Coronavirus main proteinase (3CLpro) structure: basis for design of anti-SARS drugs. *Science* **2003**, *300* (5626), 1763−7.
(24) La Monica, G.; Bono, A.; Lauria, A.; Martorana, A. Targeting SARS-CoV-2 Main Protease for Treatment of COVID-19: Covalent Inhibitors Structure-Activity Relationship Insights and Evolution Perspectives. *J. Med. Chem.* **2022**, *65* (19), 12500−12534.
(25) Chuck, C. P.; Chow, H. F.; Wan, D. C.; Wong, K. B. Profiling of substrate specificities of 3C-like proteases from group 1, 2a, 2b, and 3 coronaviruses. *PLoS One* **2011**, *6* (11), e27228.

(26) Rut, W.; Groborz, K.; Zhang, L.; Sun, X.; Zmudzinski, M.; Pawlik, B.; Wang, X.; Jochmans, D.; Neyts, J.; Młynarski, W.; Hilgenfeld, R.; Drag, M. SARS-CoV-2 Mpro inhibitors and activity-based probes for patient-sample imaging. *Nat Chem Biol* **2021**, *17*, 222.
(27) Yang, H.; Yang, M.; Ding, Y.; Liu, Y.; Lou, Z.; Zhou, Z.; Sun, L.; Mo, L.; Ye, S.; Pang, H.; Gao, G. F.; Anand, K.; Bartlam, M.; Hilgenfeld, R.; Rao, Z. The crystal structures of severe acute respiratory syndrome virus main protease and its complex with an inhibitor. *Proc. Natl. Acad. Sci. U. S. A.* **2003**, *100* (23), 13190−5.
(28) Świderek, K.; Moliner, V. Revealing the molecular mechanisms of proteolysis of SARS-CoV-2 M(pro) by QM/MM computational methods. *Chem. Sci.* **2020**, *11* (39), 10626−10630.
(29) Owen, D. R.; Allerton, C. M. N.; Anderson, A. S.; Aschenbrenner, L.; Avery, M.; Berritt, S.; Boras, B.; Cardin, R. D.; Carlo, A.; Coffman, K. J.; Dantonio, A.; Di, L.; Eng, H.; Ferre, R.; Gajiwala, K. S.; Gibson, S. A.; Greasley, S. E.; Hurst, B. L.; Kadar, E. P.; Kalgutkar, A. S.; Lee, J. C.; Lee, J.; Liu, W.; Mason, S. W.; Noell, S.; Novak, J. J.; Obach, R. S.; Ogilvie, K.; Patel, N. C.; Pettersson, M.; Rai, D. K.; Reese, M. R.; Sammons, M. F.; Sathish, J. G.; Singh, R. S. P.; Steppan, C. M.; Stewart, A. E.; Tuttle, J. B.; Updyke, L.; Verhoest, P. R.; Wei, L.; Yang, Q.; Zhu, Y. An oral SARS-CoV-2 M(pro) inhibitor clinical candidate for the treatment of COVID-19. *Science* **2021**, *374* (6575), 1586−1593.
(30) Lamb, Y. N. Nirmatrelvir Plus Ritonavir: First Approval. *Drugs* **2022**, *82* (5), 585−591.
(31) Hammond, J.; Leister-Tebbe, H.; Gardner, A.; Abreu, P.; Bao, W.; Wisemandle, W.; Baniecki, M.; Hendrick, V. M.; Damle, B.; Simón-Campos, A.; Pypstra, R.; Rusnak, J. M. Oral Nirmatrelvir for High-Risk, Nonhospitalized Adults with Covid-19. *N Engl J. Med.* **2022**, *386* (15), 1397−1408.
(32) McDonald, E. G.; Lee, T. C. Nirmatrelvir-ritonavir for COVID-19. *Cmaj* **2022**, *194* (6), E218.
(33) Charness, M. E.; Gupta, K.; Stack, G.; Strymish, J.; Adams, E.; Lindy, D. C.; Mohri, H.; Ho, D. D. Rebound of SARS-CoV-2 Infection after Nirmatrelvir-Ritonavir Treatment. *N Engl J. Med.* **2022**, *387* (11), 1045−1047.
(34) Iketani, S.; Mohri, H.; Culbertson, B.; Hong, S. J.; Duan, Y.; Luck, M. I.; Annavajhala, M. K.; Guo, Y.; Sheng, Z.; Uhlemann, A. C.; Goff, S. P.; Sabo, Y.; Yang, H.; Chavez, A.; Ho, D. D. Multiple pathways for SARS-CoV-2 resistance to nirmatrelvir. *Nature* **2023**, *613* (7944), 558−564.
(35) Yang, K. S.; Leeuwon, S. Z.; Xu, S.; Liu, W. R. Evolutionary and Structural Insights about Potential SARS-CoV-2 Evasion of Nirmatrelvir. *J. Med. Chem.* **2022**, *65* (13), 8686−8698.
(36) Jiang, X.; Su, H.; Shang, W.; Zhou, F.; Zhang, Y.; Zhao, W.; Zhang, Q.; Xie, H.; Jiang, L.; Nie, T.; Yang, F.; Xiong, M.; Huang, X.; Li, M.; Chen, P.; Peng, S.; Xiao, G.; Jiang, H.; Tang, R.; Zhang, L.; Shen, J.; Xu, Y. Structure-based development and preclinical evaluation of the SARS-CoV-2 3C-like protease inhibitor simnotrelvir. *Nat. Commun.* **2023**, *14* (1), 6463.
(37) Wang, F.; Xiao, W.; Tang, Y.; Cao, M.; Shu, D.; Asakawa, T.; Xu, Y.; Jiang, X.; Zhang, L.; Wang, W.; Tang, J.; Huang, Y.; Yang, Y.; Yang, Y.; Tang, R.; Shen, J.; Lu, H. Efficacy and safety of SIM0417 (SSD8432) plus ritonavir for COVID-19 treatment: a randomised, double-blind, placebo-controlled, phase 1b trial. *Lancet Reg Health West Pac* **2023**, *38*, 100835.
(38) Cao, B.; Wang, Y.; Lu, H.; Huang, C.; Yang, Y.; Shang, L.; Chen, Z.; Jiang, R.; Liu, Y.; Lin, L.; Peng, P.; Wang, F.; Gong, F.; Hu, H.; Cheng, C.; Yao, X.; Ye, X.; Zhou, H.; Shen, Y.; Liu, C.; Wang, C.; Yi, Z.; Hu, B.; Xu, J.; Gu, X.; Shen, J.; Xu, Y.; Zhang, L.; Fan, J.; Tang, R.; Wang, C. Oral Simnotrelvir for Adult Patients with Mild-to-Moderate Covid-19. *N Engl J. Med.* **2024**, *390* (3), 230.
(39) Unoh, Y.; Uehara, S.; Nakahara, K.; Nobori, H.; Yamatsu, Y.; Yamamoto, S.; Maruyama, Y.; Taoda, Y.; Kasamatsu, K.; Suto, T.; Kouki, K.; Nakahashi, A.; Kawashima, S.; Sanaki, T.; Toba, S.; Uemura, K.; Mizutare, T.; Ando, S.; Sasaki, M.; Orba, Y.; Sawa, H.; Sato, A.; Sato, T.; Kato, T.; Tachibana, Y. Discovery of S-217622, a Noncovalent Oral SARS-CoV-2 3CL Protease Inhibitor Clinical Candidate for Treating COVID-19. *J. Med. Chem.* **2022**, *65* (9), 6499−6512.
(40) Mukae, H.; Yotsuyanagi, H.; Ohmagari, N.; Doi, Y.; Sakaguchi, H.; Sonoyama, T.; Ichihashi, G.; Sanaki, T.; Baba, K.; Tsuge, Y.; Uehara, T. Efficacy and Safety of Ensitrelvir in Patients With Mild-to-Moderate Coronavirus Disease 2019: The Phase 2b Part of a Randomized, Placebo-Controlled, Phase 2/3 Study. *Clin Infect Dis* **2023**, *76* (8), 1403−1411.
(41) Yotsuyanagi, H.; Ohmagari, N.; Doi, Y.; Yamato, M.; Bac, N. H.; Cha, B. K.; Imamura, T.; Sonoyama, T.; Ichihashi, G.; Sanaki, T.; Tsuge, Y.; Uehara, T.; Mukae, H. Efficacy and Safety of 5-Day Oral Ensitrelvir for Patients With Mild to Moderate COVID-19: The SCORPIO-SR Randomized Clinical Trial. *JAMA Network Open* **2024**, *7* (2), e2354991−e2354991.
(42) Chen, X.; Huang, X.; Ma, Q.; Kuzmič, P.; Zhou, B.; Xu, J.; Liu, B.; Jiang, H.; Zhang, W.; Yang, C.; Wu, S.; Huang, J.; Li, H.; Long, C.; Zhao, X.; Xu, H.; Sheng, Y.; Guo, Y.; Niu, C.; Xue, L.; Xu, Y.; Liu, J.; Zhang, T.; Spencer, J.; Deng, W.; Chen, S.-H.; Xiong, X.; Yang, Z.; Zhong, N. Inhibition mechanism and antiviral activity of an α-ketoamide based SARS-CoV-2 main protease inhibitor. *bioRxiv* **2023**, DOI: 10.1101/2023.03.09.531862.
(43) Lu, H.; Zhang, G.; Mao, J.; Chen, X.; Zhan, Y.; Lin, L.; Zhang, T.; Tang, Y.; Lin, F.; Zhu, F.; Lin, Y.; Zeng, Y.; Zhang, K.; Yuan, W.; Liang, Z.; Sun, R.; Huo, L.; Hu, P.; Lin, Y.; Zhuang, X.; Wei, Z.; Chen, X.; Yan, W.; Yan, X.; Mu, L.; Lin, Z.; Tu, X.; Tan, H.; Huang, F.; Hu, Z.; Li, H.; Li, G.; Fu, H.; Yang, Z.; Chen, X.; Wang, F. S.; Zhong, N. Efficacy and safety of GST-HG171 in adult patients with mild to moderate COVID-19: a randomised, double-blind, placebo-controlled phase 2/3 trial. *EClinicalMedicine* **2024**, *71*, 102582.
(44) Zhang, H.; Zhou, J.; Chen, H.; Mao, J.; Tang, Y.; Yan, W.; Zhang, T.; Li, C.; Chen, S.; Li, G.; Zhang, G.; Ding, Y.; Liu, L. Phase I study, and dosing regimen selection for a pivotal COVID-19 trial of GST-HG171. *Antimicrob. Agents Chemother.* **2024**, *68* (1), No. e0111523.
(45) Zhang, G.; Mao, J.; He, H.; Xu, K.; Zhou, J.; Yang, Y.; Li, P.; Du, Y.; Zhang, H.; Chen, S.; Lei, W.; Lin, Y.; Chen, H.; Wang, Z.; Tang, Y.; Yan, W.; Yang, X.; Liang, Z.; Li, J.; Zhu, S.; Zhang, T.; Li, C.; Lin, J.; Yan, X.; Tan, H.; Li, H.; Li, G.; Fu, H.; Yuan, W.; Chen, X.; Yang, Z.; Chen, X.; Ding, Y.; Chen, S.; Lu, H.; Wu, G.; Zhong, N. Discovery of GST-HG171, A Potent and Selective Oral 3CL Protease Inhibitor for the Treatment of COVID-19. *SM J. Infect Dis.* **2023**, *6*, 1−9 https://www.jsmcentral.org/sm-infectious-diseases/smjid685562.pdf.
(46) Hou, N.; Shuai, L.; Zhang, L.; Xie, X.; Tang, K.; Zhu, Y.; Yu, Y.; Zhang, W.; Tan, Q.; Zhong, G.; Wen, Z.; Wang, C.; He, X.; Huo, H.; Gao, H.; Xu, Y.; Xue, J.; Peng, C.; Zou, J.; Schindewolf, C.; Menachery, V.; Su, W.; Yuan, Y.; Shen, Z.; Zhang, R.; Yuan, S.; Yu, H.; Shi, P. Y.; Bu, Z.; Huang, J.; Hu, Q. Development of Highly Potent Noncovalent Inhibitors of SARS-CoV-2 3CLpro. *ACS Cent Sci.* **2023**, *9* (2), 217−227.
(47) Zhang, L.; Xie, X.; Luo, H.; Qian, R.; Yang, Y.; Yu, H.; Huang, J.; Shi, P. Y.; Hu, Q. Resistance mechanisms of SARS-CoV-2 3CLpro to the non-covalent inhibitor WU-04. *Cell Discov* **2024**, *10* (1), 40.
(48) Shang, W.; Dai, W.; Yao, C.; Xu, L.; Tao, X.; Su, H.; Li, J.; Xie, X.; Xu, Y.; Hu, M.; Xie, D.; Jiang, H.; Zhang, L.; Liu, H. In vitro and in vivo evaluation of the main protease inhibitor FB2001 against SARS-CoV-2. *Antiviral Res.* **2022**, *208*, 105450.
(49) Li, H.; Li, J.; Li, J.; Li, H.; Wang, X.; Jiang, J.; Lei, L.; Sun, H.; Tang, M.; Dong, B.; He, W.; Si, S.; Hong, B.; Li, Y.; Song, D.; Peng, Z.; Che, Y.; Jiang, J.-D. Carrimycin inhibits coronavirus replication by decreasing the efficiency of programmed − 1 ribosomal frameshifting through directly binding to the RNA pseudoknot of viral frameshift-stimulatory element. *Acta Pharmaceutica Sinica B* **2024**, *14*, 2567.
(50) Shih, P. C.; Mao, Y. W.; Hu, J. W.; Hsieh, H. Y.; Shih, T. M.; Lu, L. P.; Chang, W. H.; Huang, C. H.; Lin, C. H.; Lin, C. H.; Tan, P.; Yang, Y. C.; Chien, M. H.; Su, C. C.; Yeh, C. H.; Chuang, P. Y.; Hsieh, T. L.; Wang, C. C.; Hsieh, P. S.; Chou, T. Y.; Tsai, G. E. Development of Ultrapure and Potent Tannic Acids as a Pan-coronal

https://doi.org/10.1021/acsomega.4c03023
ACS Omega 2024, 9, 34196−34219

Antiviral Therapeutic. *ACS Pharmacol Transl Sci.* **2022**, *5* (6), 400−412.
(51) Drayman, N.; DeMarco, J. K.; Jones, K. A.; Azizi, S. A.; Froggatt, H. M.; Tan, K.; Maltseva, N. I.; Chen, S.; Nicolaescu, V.; Dvorkin, S.; Furlong, K.; Kathayat, R. S.; Firpo, M. R.; Mastrodomenico, V.; Bruce, E. A.; Schmidt, M. M.; Jedrzejczak, R.; Muñoz-Alía, M.; Schuster, B.; Nair, V.; Han, K. Y.; O'Brien, A.; Tomatsidou, A.; Meyer, B.; Vignuzzi, M.; Missiakas, D.; Botten, J. W.; Brooke, C. B.; Lee, H.; Baker, S. C.; Mounce, B. C.; Heaton, N. S.; Severson, W. E.; Palmer, K. E.; Dickinson, B. C.; Joachimiak, A.; Randall, G.; Tay, S. Masitinib is a broad coronavirus 3CL inhibitor that blocks replication of SARS-CoV-2. *Science* **2021**, *373* (6557), 931−936.
(52) Li, Y.; Zang, T. I.; Xu, L.; Leonard, D.; Hoang, K.; Greizer, T.; Zhang, S.; Foster, C.; Huang, M.; Kibel, J.; Klaene, J.; Or, Y. S.; Jiang, L.-J. 1123. EDP-235, A Potent and Once-daily Oral Antiviral, Demonstrates Excellent Penetration into Macrophages and Monocytes, with the Potential for Mitigation of Cytokine Storm in High-Risk COVID-19 Patients. *Open Forum Infectious Diseases* **2022**, DOI: 10.1093/ofid/ofac492.962.
(53) Allerton, C. M. N.; Arcari, J. T.; Aschenbrenner, L. M.; Avery, M.; Bechle, B. M.; Behzadi, M. A.; Boras, B.; Buzon, L. M.; Cardin, R. D.; Catlin, N. R.; Carlo, A. A.; Coffman, K. J.; Dantonio, A.; Di, L.; Eng, H.; Farley, K. A.; Ferre, R. A.; Gernhardt, S. S.; Gibson, S. A.; Greasley, S. E.; Greenfield, S. R.; Hurst, B. L.; Kalgutkar, A. S.; Kimoto, E.; Lanyon, L. F.; Lovett, G. H.; Lian, Y.; Liu, W.; Martínez Alsina, L. A.; Noell, S.; Obach, R. S.; Owen, D. R.; Patel, N. C.; Rai, D. K.; Reese, M. R.; Rothan, H. A.; Sakata, S.; Sammons, M. F.; Sathish, J. G.; Sharma, R.; Steppan, C. M.; Tuttle, J. B.; Verhoest, P. R.; Wei, L.; Yang, Q.; Yurgelonis, I.; Zhu, Y. A Second-Generation Oral SARS-CoV-2 Main Protease Inhibitor Clinical Candidate for the Treatment of COVID-19. *J. Med. Chem.* **2024**, DOI: 10.1021/acs.jmedchem.3c02469.
(54) Mao, L.; Shaabani, N.; Zhang, X.; Jin, C.; Xu, W.; Argent, C.; Kushnareva, Y.; Powers, C.; Stegman, K.; Liu, J.; Xie, H.; Xu, C.; Bao, Y.; Xu, L.; Zhang, Y.; Yang, H.; Qian, S.; Hu, Y.; Shao, J.; Zhang, C.; Li, T.; Li, Y.; Liu, N.; Lin, Z.; Wang, S.; Wang, C.; Shen, W.; Lin, Y.; Shu, D.; Zhu, Z.; Kotoi, O.; Kerwin, L.; Han, Q.; Chumakova, L.; Teijaro, J.; Royal, M.; Brunswick, M.; Allen, R.; Ji, H.; Lu, H.; Xu, X. Olgotrelvir, a dual inhibitor of SARS-CoV-2 Mpro and cathepsin L, as a standalone antiviral oral intervention candidate for COVID-19. *Med.* **2024**, *5* (1), 42−61.
(55) Wang, H.; Chen, M.; Zhang, X.; Xie, S.; Qin, J.; Li, J. Peptide-based PROTACs: Current Challenges and Future Perspectives. *Curr. Med. Chem.* **2024**, *31* (2), 208−222.
(56) Pillaiyar, T.; Manickam, M.; Namasivayam, V.; Hayashi, Y.; Jung, S. H. An Overview of Severe Acute Respiratory Syndrome-Coronavirus (SARS-CoV) 3CL Protease Inhibitors: Peptidomimetics and Small Molecule Chemotherapy. *J. Med. Chem.* **2016**, *59* (14), 6595−628.
(57) Huang, C.; Shuai, H.; Qiao, J.; Hou, Y.; Zeng, R.; Xia, A.; Xie, L.; Fang, Z.; Li, Y.; Yoon, C.; Huang, Q.; Hu, B.; You, J.; Quan, B.; Zhao, X.; Guo, N.; Zhang, S.; Ma, R.; Zhang, J.; Wang, Y.; Yang, R.; Zhang, S.; Nan, J.; Xu, H.; Wang, F.; Lei, J.; Chu, H.; Yang, S. A new generation M(pro) inhibitor with potent activity against SARS-CoV-2 Omicron variants. *Signal Transduct Target Ther* **2023**, *8* (1), 128.
(58) Shurtleff, V. W.; Layton, M. E.; Parish, C. A.; Perkins, J. J.; Schreier, J. D.; Wang, Y.; Adam, G. C.; Alvarez, N.; Bahmanjah, S.; Bahnck-Teets, C. M.; Boyce, C. W.; Burlein, C.; Cabalu, T. D.; Campbell, B. T.; Carroll, S. S.; Chang, W.; de Lera Ruiz, M.; Dolgov, E.; Fay, J. F.; Fox, N. G.; Goh, S. L.; Hartingh, T. J.; Hurzy, D. M.; Kelly, M. J., 3rd; Klein, D. J.; Klingler, F. M.; Krishnamurthy, H.; Kudalkar, S.; Mayhood, T. W.; McKenna, P. M.; Murray, E. M.; Nahas, D.; Nawrat, C. C.; Park, S.; Qian, D.; Roecker, A. J.; Sharma, V.; Shipe, W. D.; Su, J.; Taggart, R. V.; Truong, Q.; Wu, Y.; Zhou, X.; Zhuang, N.; Perlin, D. S.; Olsen, D. B.; Howe, J. A.; McCauley, J. A. Invention of MK-7845, a SARS-CoV-2 3CL Protease Inhibitor Employing a Novel Difluorinated Glutamine Mimic. *J. Med. Chem.* **2024**, *67* (5), 3935−3958.
(59) Zhang, L.; Lin, D.; Kusov, Y.; Nian, Y.; Ma, Q.; Wang, J.; von Brunn, A.; Leyssen, P.; Lanko, K.; Neyts, J.; de Wilde, A.; Snijder, E. J.; Liu, H.; Hilgenfeld, R. α-Ketoamides as Broad-Spectrum Inhibitors of Coronavirus and Enterovirus Replication: Structure-Based Design, Synthesis, and Activity Assessment. *Journal of medicinal chemistry* **2020**, *63* (9), 4562−4578.
(60) Zhang, L.; Lin, D.; Sun, X.; Curth, U.; Drosten, C.; Sauerhering, L.; Becker, S.; Rox, K.; Hilgenfeld, R. Crystal structure of SARS-CoV-2 main protease provides a basis for design of improved α-ketoamide inhibitors. *Science (New York, N.Y.)* **2020**, *368* (6489), 409−412.
(61) Pelliccia, S.; Cerchia, C.; Esposito, F.; Cannalire, R.; Corona, A.; Costanzi, E.; Kuzikov, M.; Gribbon, P.; Zaliani, A.; Brindisi, M.; Storici, P.; Tramontano, E.; Summa, V. Easy access to α-ketoamides as SARS-CoV-2 and MERS M(pro) inhibitors via the PADAM oxidation route. *European journal of medicinal chemistry* **2022**, *244*, 114853.
(62) Hoffman, R. L.; Kania, R. S.; Brothers, M. A.; Davies, J. F.; Ferre, R. A.; Gajiwala, K. S.; He, M.; Hogan, R. J.; Kozminski, K.; Li, L. Y.; Lockner, J. W.; Lou, J.; Marra, M. T.; Mitchell, L. J., Jr.; Murray, B. W.; Nieman, J. A.; Noell, S.; Planken, S. P.; Rowe, T.; Ryan, K.; Smith, G. J., 3rd; Solowiej, J. E.; Steppan, C. M.; Taggart, B. Discovery of Ketone-Based Covalent Inhibitors of Coronavirus 3CL Proteases for the Potential Therapeutic Treatment of COVID-19. *J. Med. Chem.* **2020**, *63* (21), 12725−12747.
(63) Dayan Elshan, N. G. R.; Wolff, K. C.; Riva, L.; Woods, A. K.; Grabovyi, G.; Wilson, K.; Pedroarena, J.; Ghorai, S.; Nazarian, A.; Weiss, F.; Liu, Y.; Mazumdar, W.; Song, L.; Okwor, N.; Malvin, J.; Bakowski, M. A.; Beutler, N.; Kirkpatrick, M. G.; Gebara-Lamb, A.; Huang, E.; Nguyen-Tran, V. T. B.; Chi, V.; Li, S.; Rogers, T. F.; McNamara, C. W.; Gupta, A. K.; Rahimi, A.; Chen, J. J.; Joseph, S. B.; Schultz, P. G.; Chatterjee, A. K. Discovery of CMX990: A Potent SARS-CoV-2 3CL Protease Inhibitor Bearing a Novel Warhead. *J. Med. Chem.* **2024**, *67* (4), 2369−2378.
(64) Dai, W.; Zhang, B.; Jiang, X. M.; Su, H.; Li, J.; Zhao, Y.; Xie, X.; Jin, Z.; Peng, J.; Liu, F.; Li, C.; Li, Y.; Bai, F.; Wang, H.; Cheng, X.; Cen, X.; Hu, S.; Yang, X.; Wang, J.; Liu, X.; Xiao, G.; Jiang, H.; Rao, Z.; Zhang, L. K.; Xu, Y.; Yang, H.; Liu, H. Structure-based design of antiviral drug candidates targeting the SARS-CoV-2 main protease. *Science* **2020**, *368* (6497), 1331−1335.
(65) Qiao, J.; Li, Y. S.; Zeng, R.; Liu, F. L.; Luo, R. H.; Huang, C.; Wang, Y. F.; Zhang, J.; Quan, B.; Shen, C.; Mao, X.; Liu, X.; Sun, W.; Yang, W.; Ni, X.; Wang, K.; Xu, L.; Duan, Z. L.; Zou, Q. C.; Zhang, H. L.; Qu, W.; Long, Y. H.; Li, M. H.; Yang, R. C.; Liu, X.; You, J.; Zhou, Y.; Yao, R.; Li, W. P.; Liu, J. M.; Chen, P.; Liu, Y.; Lin, G. F.; Yang, X.; Zou, J.; Li, L.; Hu, Y.; Lu, G. W.; Li, W. M.; Wei, Y. Q.; Zheng, Y. T.; Lei, J.; Yang, S. SARS-CoV-2 M(pro) inhibitors with antiviral activity in a transgenic mouse model. *Science* **2021**, *371* (6536), 1374−1378.
(66) Wang, H.; Pei, R.; Li, X.; Deng, W.; Xing, S.; Zhang, Y.; Zhang, C.; He, S.; Sun, H.; Xiao, S.; Xiong, J.; Zhang, Y.; Chen, X.; Wang, Y.; Guo, Y.; Zhang, B.; Shang, L. The structure-based design of peptidomimetic inhibitors against SARS-CoV-2 3C like protease as Potent anti-viral drug candidate. *European journal of medicinal chemistry* **2022**, *238*, 114458.
(67) Wang, Y.; Xu, B.; Ma, S.; Wang, H.; Shang, L.; Zhu, C.; Ye, S. Discovery of SARS-CoV-2 3CL(Pro) Peptidomimetic Inhibitors through the Catalytic Dyad Histidine-Specific Protein-Ligand Interactions. *International journal of molecular sciences* **2022**, *23* (4), 2392.
(68) Stille, J. K.; Tjutrins, J.; Wang, G.; Venegas, F. A.; Hennecker, C.; Rueda, A. M.; Sharon, I.; Blaine, N.; Miron, C. E.; Pinus, S.; Labarre, A.; Plescia, J.; Burai Patrascu, M.; Zhang, X.; Wahba, A. S.; Vlaho, D.; Huot, M. J.; Schmeing, T. M.; Mittermaier, A. K.; Moitessier, N. Design, synthesis and in vitro evaluation of novel SARS-CoV-2 3CL(pro) covalent inhibitors. *Eur. J. Med. Chem.* **2022**, *229*, 114046.
(69) Ma, C.; Xia, Z.; Sacco, M. D.; Hu, Y.; Townsend, J. A.; Meng, X.; Choza, J.; Tan, H.; Jang, J.; Gongora, M. V.; Zhang, X.; Zhang, F.;

https://doi.org/10.1021/acsomega.4c03023
ACS Omega 2024, 9, 34196−34219

Xiang, Y.; Marty, M. T.; Chen, Y.; Wang, J. Discovery of Di- and Trihaloacetamides as Covalent SARS-CoV-2 Main Protease Inhibitors with High Target Specificity. *J. Am. Chem. Soc.* **2021**, *143* (49), 20697−20709.
(70) Hirose, Y.; Shindo, N.; Mori, M.; Onitsuka, S.; Isogai, H.; Hamada, R.; Hiramoto, T.; Ochi, J.; Takahashi, D.; Ueda, T.; Caaveiro, J. M. M.; Yoshida, Y.; Ohdo, S.; Matsunaga, N.; Toba, S.; Sasaki, M.; Orba, Y.; Sawa, H.; Sato, A.; Kawanishi, E.; Ojida, A. Discovery of Chlorofluoroacetamide-Based Covalent Inhibitors for Severe Acute Respiratory Syndrome Coronavirus 2 3CL Protease. *J. Med. Chem.* **2022**, *65* (20), 13852−13865.
(71) Liu, M.; Li, J.; Liu, W.; Yang, Y.; Zhang, M.; Ye, Y.; Zhu, W.; Zhou, C.; Zhai, H.; Xu, Z.; Zhang, G.; Huang, H. The S1′-S3′ Pocket of the SARS-CoV-2 Main Protease Is Critical for Substrate Selectivity and Can Be Targeted with Covalent Inhibitors. *Angew. Chem., Int. Ed. Engl.* **2023**, *62*, e202309657.
(72) Khatua, K.; Alugubelli, Y. R.; Yang, K. S.; Vulupala, V. R.; Blankenship, L. R.; Coleman, D.; Atla, S.; Chaki, S. P.; Geng, Z. Z.; Ma, X. R.; Xiao, J.; Chen, P.-H.; Cho, C.-C. D.; Sharma, S.; Vatansever, E. C.; Ma, Y.; Yu, G.; Neuman, B. W.; Xu, S.; Liu, W. R. Azapeptides with unique covalent warheads as SARS-CoV-2 main protease inhibitors. *Antiviral Res.* **2024**, *225*, 105874.
(73) Kim, Y.; Lovell, S.; Tiew, K. C.; Mandadapu, S. R.; Alliston, K. R.; Battaile, K. P.; Groutas, W. C.; Chang, K. O. Broad-spectrum antivirals against 3C or 3C-like proteases of picornaviruses, noroviruses, and coronaviruses. *J. Virol* **2012**, *86* (21), 11754−62.
(74) Hung, H. C.; Ke, Y. Y.; Huang, S. Y.; Huang, P. N.; Kung, Y. A.; Chang, T. Y.; Yen, K. J.; Peng, T. T.; Chang, S. E.; Huang, C. T.; Tsai, Y. R.; Wu, S. H.; Lee, S. J.; Lin, J. H.; Liu, B. S.; Sung, W. C.; Shih, S. R.; Chen, C. T.; Hsu, J. T. Discovery of M Protease Inhibitors Encoded by SARS-CoV-2. *Antimicrob. Agents Chemother.* **2020**, DOI: 10.1128/AAC.00872-20.
(75) Cáceres, C. J.; Cardenas-Garcia, S.; Carnaccini, S.; Seibert, B.; Rajao, D. S.; Wang, J.; Perez, D. R. Efficacy of GC-376 against SARS-CoV-2 virus infection in the K18 hACE2 transgenic mouse model. *Sci. Rep* **2021**, *11* (1), 9609.
(76) Joaquín Cáceres, C.; Cardenas-Garcia, S.; Carnaccini, S.; Seibert, B.; Rajao, D. S.; Wang, J.; Perez, D. R. Efficacy of GC-376 against SARS-CoV-2 virus infection in the K18 hACE2 transgenic mouse model. *Sci. Rep.* **2021**, DOI: 10.1038/s41598-021-89013-w.
(77) Arutyunova, E.; Khan, M. B.; Fischer, C.; Lu, J.; Lamer, T.; Vuong, W.; van Belkum, M. J.; McKay, R. T.; Tyrrell, D. L.; Vederas, J. C.; Young, H. S.; Lemieux, M. J. N-Terminal Finger Stabilizes the S1 Pocket for the Reversible Feline Drug GC376 in the SARS-CoV-2 M(pro) Dimer. *J. Mol. Biol.* **2021**, *433* (13), 167003.
(78) Kim, Y.; Mandadapu, S. R.; Groutas, W. C.; Chang, K. O. Potent inhibition of feline coronaviruses with peptidyl compounds targeting coronavirus 3C-like protease. *Antiviral research* **2013**, *97* (2), 161−8.
(79) Liu, H.; Iketani, S.; Zask, A.; Khanizeman, N.; Bednarova, E.; Forouhar, F.; Fowler, B.; Hong, S. J.; Mohri, H.; Nair, M. S.; Huang, Y.; Tay, N. E. S.; Lee, S.; Karan, C.; Resnick, S. J.; Quinn, C.; Li, W.; Shion, H.; Xia, X.; Daniels, J. D.; Bartolo-Cruz, M.; Farina, M.; Rajbhandari, P.; Jurtschenko, C.; Lauber, M. A.; McDonald, T.; Stokes, M. E.; Hurst, B. L.; Rovis, T.; Chavez, A.; Ho, D. D.; Stockwell, B. R. Development of optimized drug-like small molecule inhibitors of the SARS-CoV-2 3CL protease for treatment of COVID-19. *Nat. Commun.* **2022**, *13* (1), 1891.
(80) Chuck, C.-P.; Chen, C.; Ke, Z.; Chi-Cheong Wan, D.; Chow, H.-F.; Wong, K.-B. Design, synthesis and crystallographic analysis of nitrile-based broad-spectrum peptidomimetic inhibitors for coronavirus 3C-like proteases. *Eur. J. Med. Chem.* **2013**, *59*, 1−6.
(81) Lea, A. P.; Faulds, D. Ritonavir. *Drugs* **1996**, *52* (4), 541−6.
(82) Duan, Y.; Zhou, H.; Liu, X.; Iketani, S.; Lin, M.; Zhang, X.; Bian, Q.; Wang, H.; Sun, H.; Hong, S. J.; Culbertson, B.; Mohri, H.; Luck, M. I.; Zhu, Y.; Liu, X.; Lu, Y.; Yang, X.; Yang, K.; Sabo, Y.; Chavez, A.; Goff, S. P.; Rao, Z.; Ho, D. D.; Yang, H. Molecular mechanisms of SARS-CoV-2 resistance to nirmatrelvir. *Nature* **2023**, *622* (7982), 376−382.
(83) Aggarwal, N. R.; Beaty, L. E.; Bennett, T. D.; Fish, L. E.; Jacobs, J. R.; Mayer, D. A.; Molina, K. C.; Peers, J. L.; Richardson, D. B.; Russell, S.; Varela, A.; Webb, B. J.; Wynia, M. K.; Xiao, M.; Carlson, N. E.; Ginde, A. A. Real-world use of nirmatrelvir-ritonavir in COVID-19 outpatients during BQ.1, BQ.1.1., and XBB.1.5 predominant omicron variants in three U.S. health systems: a retrospective cohort study. *Lancet Reg Health Am.* **2024**, *31*, 100693.
(84) Zhong, B.; Peng, W.; Du, S.; Chen, B.; Feng, Y.; Hu, X.; Lai, Q.; Liu, S.; Zhou, Z. W.; Fang, P.; Wu, Y.; Gao, F.; Zhou, H.; Sun, L. Oridonin Inhibits SARS-CoV-2 by Targeting Its 3C-Like Protease. *Small Sci.* **2022**, *2* (6), 2270012.
(85) Iketani, S.; Mohri, H.; Culbertson, B.; Hong, S. J.; Duan, Y.; Luck, M. I.; Annavajhala, M. K.; Guo, Y.; Sheng, Z.; Uhlemann, A. C.; Goff, S. P.; Sabo, Y.; Yang, H.; Chavez, A.; Ho, D. D. Multiple pathways for SARS-CoV-2 resistance to nirmatrelvir. *Nature* **2023**, *613*, 558.
(86) Kneller, D. W.; Li, H.; Phillips, G.; Weiss, K. L.; Zhang, Q.; Arnould, M. A.; Jonsson, C. B.; Surendranathan, S.; Parvathareddy, J.; Blakeley, M. P.; Coates, L.; Louis, J. M.; Bonnesen, P. V.; Kovalevsky, A. Covalent narlaprevir- and boceprevir-derived hybrid inhibitors of SARS-CoV-2 main protease. *Nat. Commun.* **2022**, *13* (1), 2268.
(87) Matsoukas, J.; Apostolopoulos, V.; Lazoura, E.; Deraos, G.; Matsoukas, M.-T.; Katsara, M.; Tselios, T.; Deraos, S. Round and Round we Go: Cyclic Peptides in Disease. *Curr. Med. Chem.* **2006**, *13* (19), 2221−2232.
(88) Clardy, J.; Walsh, C. Lessons from natural molecules. *Nature* **2004**, *432* (7019), 829−837.
(89) Qian, Z.; Rhodes, C. A.; McCroskey, L. C.; Wen, J.; Appiah-Kubi, G.; Wang, D. J.; Guttridge, D. C.; Pei, D. Enhancing the Cell Permeability and Metabolic Stability of Peptidyl Drugs by Reversible Bicyclization. *Angew. Chem., Int. Ed.* **2017**, *56* (6), 1525−1529.
(90) Kreutzer, A. G.; Krumberger, M.; Diessner, E. M.; Parrocha, C. M. T.; Morris, M. A.; Guaglianone, G.; Butts, C. T.; Nowick, J. S. A cyclic peptide inhibitor of the SARS-CoV-2 main protease. *Eur. J. Med. Chem.* **2021**, *221*, 113530.
(91) Johansen-Leete, J.; Ullrich, S.; Fry, S. E.; Frkic, R.; Bedding, M. J.; Aggarwal, A.; Ashhurst, A. S.; Ekanayake, K. B.; Mahawaththa, M. C.; Sasi, V. M.; Luedtke, S.; Ford, D. J.; O'Donoghue, A. J.; Passioura, T.; Larance, M.; Otting, G.; Turville, S.; Jackson, C. J.; Nitsche, C.; Payne, R. J. Antiviral cyclic peptides targeting the main protease of SARS-CoV-2. *Chem. Sci.* **2022**, *13* (13), 3826−3836.
(92) Miura, T.; Malla, T. R.; Owen, C. D.; Tumber, A.; Brewitz, L.; McDonough, M. A.; Salah, E.; Terasaka, N.; Katoh, T.; Lukacik, P.; Strain-Damerell, C.; Mikolajek, H.; Walsh, M. A.; Kawamura, A.; Schofield, C. J.; Suga, H. In vitro selection of macrocyclic peptide inhibitors containing cyclic γ(2,4)-amino acids targeting the SARS-CoV-2 main protease. *Nat. Chem.* **2023**, *15* (7), 998−1005.
(93) Tedesco, F.; Calugi, L.; Lenci, E.; Trabocchi, A. Peptidomimetic Small-Molecule Inhibitors of 3CLPro Activity and Spike-ACE2 Interaction: Toward Dual-Action Molecules against Coronavirus Infections. *J. Org. Chem.* **2022**, *87* (18), 12041−12051.
(94) Azevedo, P.; Camargo, P. G.; Constant, L. E. C.; Costa, S. D. S.; Silva, C. S.; Rosa, A. S.; Souza, D. D. C.; Tucci, A. R.; Ferreira, V. N. S.; Oliveira, T. K. F.; Borba, N. R. R.; Rodrigues, C. R.; Albuquerque, M. G.; Dias, L. R. S.; Garrett, R.; Miranda, M. D.; Allonso, D.; Lima, C.; Muri, E. M. F. Statine-based peptidomimetic compounds as inhibitors for SARS-CoV-2 main protease (SARS-CoV-2 Mpro). *Sci. Rep* **2024**, *14* (1), 8991.
(95) Xiao, Y. Q.; Long, J.; Zhang, S. S.; Zhu, Y. Y.; Gu, S. X. Non-peptidic inhibitors targeting SARS-CoV-2 main protease: A review. *Bioorg Chem.* **2024**, *147*, 107380.
(96) Song, L.; Gao, S.; Ye, B.; Yang, M.; Cheng, Y.; Kang, D.; Yi, F.; Sun, J. P.; Menéndez-Arias, L.; Neyts, J.; Liu, X.; Zhan, P. Medicinal chemistry strategies towards the development of non-covalent SARS-CoV-2 Mpro inhibitors. *Acta Pharm. Sin B* **2024**, *14* (1), 87−109.
(97) Jin, Z.; Du, X.; Xu, Y.; Deng, Y.; Liu, M.; Zhao, Y.; Zhang, B.; Li, X.; Zhang, L.; Peng, C.; Duan, Y.; Yu, J.; Wang, L.; Yang, K.; Liu, F.; Jiang, R.; Yang, X.; You, T.; Liu, X.; Yang, X.; Bai, F.; Liu, H.; Liu, X.; Guddat, L. W.; Xu, W.; Xiao, G.; Qin, C.; Shi, Z.; Jiang, H.; Rao,

https://doi.org/10.1021/acsomega.4c03023
ACS Omega 2024, 9, 34196−34219

Z.; Yang, H. Structure of M(pro) from SARS-CoV-2 and discovery of its inhibitors. *Nature* **2020**, *582* (7811), 289−293.
(98) Menéndez, C. A.; Byléhn, F.; Perez-Lemus, G. R.; Alvarado, W.; de Pablo, J. J. Molecular characterization of ebselen binding activity to SARS-CoV-2 main protease. *Sci. Adv.* **2020**, DOI: 10.1126/sciadv.abd0345.
(99) Sun, L. Y.; Chen, C.; Su, J.; Li, J. Q.; Jiang, Z.; Gao, H.; Chigan, J. Z.; Ding, H. H.; Zhai, L.; Yang, K. W. Ebsulfur and Ebselen as highly potent scaffolds for the development of potential SARS-CoV-2 antivirals. *Bioorganic chemistry* **2021**, *112*, 104889.
(100) Gurard-Levin, Z. A.; Liu, C.; Jekle, A.; Jaisinghani, R.; Ren, S.; Vandyck, K.; Jochmans, D.; Leyssen, P.; Neyts, J.; Blatt, L. M.; Beigelman, L.; Symons, J. A.; Raboisson, P.; Scholle, M. D.; Deval, J. Evaluation of SARS-CoV-2 3C-like protease inhibitors using self-assembled monolayer desorption ionization mass spectrometry. *Antiviral Res.* **2020**, *182*, 104924.
(101) Ma, C.; Hu, Y.; Townsend, J. A.; Lagarias, P. I.; Marty, M. T.; Kolocouris, A.; Wang, J. Ebselen, Disulfiram, Carmofur, PX-12, Tideglusib, and Shikonin Are Nonspecific Promiscuous SARS-CoV-2 Main Protease Inhibitors. *ACS Pharmacol Transl Sci.* **2020**, *3* (6), 1265−1277.
(102) Ma, C.; Tan, H.; Choza, J.; Wang, Y.; Wang, J. Validation and invalidation of SARS-CoV-2 main protease inhibitors using the Flip-GFP and Protease-Glo luciferase assays. *Acta Pharm. Sin B* **2022**, *12* (4), 1636−1651.
(103) Tan, H.; Ma, C.; Wang, J. Invalidation of dieckol and 1,2,3,4,6-pentagalloylglucose (PGG) as SARS-CoV-2 main protease inhibitors and the discovery of PGG as a papain-like protease inhibitor. *Res. Sq* **2022**, *31*, 1147.
(104) Karges, J.; Kalaj, M.; Gembicky, M.; Cohen, S. M. Re(I) Tricarbonyl Complexes as Coordinate Covalent Inhibitors for the SARS-CoV-2 Main Cysteine Protease. *Angewandte Chemie (International ed. in English)* **2021**, *60* (19), 10716−10723.
(105) DeLaney, C.; Sheng, Y.; Pectol, D. C.; Vantansever, E.; Zhang, H.; Bhuvanesh, N.; Salas, I.; Liu, W. R.; Fierke, C. F.; Darensbourg, M. Y. Zinc thiotropolone combinations as inhibitors of the SARS-CoV-2 main protease. *Dalton transactions (Cambridge, England: 2003)* **2021**, *50* (35), 12226−12233.
(106) Panchariya, L.; Khan, W. A.; Kuila, S.; Sonkar, K.; Sahoo, S.; Ghoshal, A.; Kumar, A.; Verma, D. K.; Hasan, A.; Khan, M. A.; Jain, N.; Mohapatra, A. K.; Das, S.; Thakur, J. K.; Maiti, S.; Nanda, R. K.; Halder, R.; Sunil, S.; Arockiasamy, A. Zinc(2+) ion inhibits SARS-CoV-2 main protease and viral replication in vitro. *Chemical communications (Cambridge, England)* **2021**, *57* (78), 10083−10086.
(107) Wang, R.; Chan, J. F.; Wang, S.; Li, H.; Zhao, J.; Ip, T. K.; Zuo, Z.; Yuen, K. Y.; Yuan, S.; Sun, H. Orally administered bismuth drug together with N-acetyl cysteine as a broad-spectrum anti-coronavirus cocktail therapy. *Chemical science* **2022**, *13* (8), 2238−2248.
(108) Dömling, A.; Ugi, I. I. Multicomponent Reactions with Isocyanides. *Angew. Chem., Int. Ed. Engl.* **2000**, *39* (18), 3168−3210.
(109) Quan, B. X.; Shuai, H.; Xia, A. J.; Hou, Y.; Zeng, R.; Liu, X. L.; Lin, G. F.; Qiao, J. X.; Li, W. P.; Wang, F. L.; Wang, K.; Zhou, R. J.; Yuen, T. T.; Chen, M. X.; Yoon, C.; Wu, M.; Zhang, S. Y.; Huang, C.; Wang, Y. F.; Yang, W.; Tian, C.; Li, W. M.; Wei, Y. Q.; Yuen, K. Y.; Chan, J. F.; Lei, J.; Chu, H.; Yang, S. An orally available M(pro) inhibitor is effective against wild-type SARS-CoV-2 and variants including Omicron. *Nat. Microbiol* **2022**, *7* (5), 716−725.
(110) Zheng, J.; Wong, L. R.; Li, K.; Verma, A. K.; Ortiz, M. E.; Wohlford-Lenane, C.; Leidinger, M. R.; Knudson, C. M.; Meyerholz, D. K.; McCray, P. B., Jr.; Perlman, S. COVID-19 treatments and pathogenesis including anosmia in K18-hACE2 mice. *Nature* **2021**, *589* (7843), 603−607.
(111) Winkler, E. S.; Bailey, A. L.; Kafai, N. M.; Nair, S.; McCune, B. T.; Yu, J.; Fox, J. M.; Chen, R. E.; Earnest, J. T.; Keeler, S. P.; Ritter, J. H.; Kang, L. I.; Dort, S.; Robichaud, A.; Head, R.; Holtzman, M. J.; Diamond, M. S. SARS-CoV-2 infection of human ACE2-transgenic mice causes severe lung inflammation and impaired function. *Nat. Immunol* **2020**, *21* (11), 1327−1335.
(112) Oladunni, F. S.; Park, J. G.; Pino, P. A.; Gonzalez, O.; Akhter, A.; Allué-Guardia, A.; Olmo-Fontánez, A.; Gautam, S.; Garcia-Vilanova, A.; Ye, C.; Chiem, K.; Headley, C.; Dwivedi, V.; Parodi, L. M.; Alfson, K. J.; Staples, H. M.; Schami, A.; Garcia, J. I.; Whigham, A.; Platt, R. N., 2nd; Gazi, M.; Martinez, J.; Chuba, C.; Earley, S.; Rodriguez, O. H.; Mdaki, S. D.; Kavelish, K. N.; Escalona, R.; Hallam, C. R. A.; Christie, C.; Patterson, J. L.; Anderson, T. J. C.; Carrion, R., Jr.; Dick, E. J., Jr.; Hall-Ursone, S.; Schlesinger, L. S.; Alvarez, X.; Kaushal, D.; Giavedoni, L. D.; Turner, J.; Martinez-Sobrido, L.; Torrelles, J. B. Lethality of SARS-CoV-2 infection in K18 human angiotensin-converting enzyme 2 transgenic mice. *Nat. Commun.* **2020**, *11* (1), 6122.
(113) Gao, S.; Song, L.; Claff, T.; Woodson, M.; Sylvester, K.; Jing, L.; Weiße, R. H.; Cheng, Y.; Sträter, N.; Schäkel, L.; Gütschow, M.; Ye, B.; Yang, M.; Zhang, T.; Kang, D.; Toth, K.; Tavis, J.; Tollefson, A. E.; Müller, C. E.; Zhan, P.; Liu, X. Discovery and Crystallographic Studies of Nonpeptidic Piperazine Derivatives as Covalent SARS-CoV-2 Main Protease Inhibitors. *J. Med. Chem.* **2022**, *65* (24), 16902−16917.
(114) Ren, P.; Yu, C.; Zhang, R.; Nie, T.; Hu, Q.; Li, H.; Zhang, X.; Zhang, X.; Li, S.; Liu, L.; Dai, W.; Li, J.; Xu, Y.; Su, H.; Zhang, L.; Liu, H.; Bai, F. Discovery, synthesis and mechanism study of 2,3,5-substituted [1,2,4]-thiadiazoles as covalent inhibitors targeting 3C-Like protease of SARS-CoV-2. *Eur. J. Med. Chem.* **2023**, *249*, 115129.
(115) Ren, P.; Li, H.; Nie, T.; Jian, X.; Yu, C.; Li, J.; Su, H.; Zhang, X.; Li, S.; Yang, X.; Peng, C.; Yin, Y.; Zhang, L.; Xu, Y.; Liu, H.; Bai, F. Discovery and Mechanism Study of SARS-CoV-2 3C-like Protease Inhibitors with a New Reactive Group. *J. Med. Chem.* **2023**, *66*, 12266.
(116) Hattori, S.-I.; Higshi-Kuwata, N.; Raghavaiah, J.; Das, D.; Bulut, H.; Davis, D. A.; Takamatsu, Y.; Matsuda, K.; Takamune, N.; Kishimoto, N.; Okamura, T.; Misumi, S.; Yarchoan, R.; Maeda, K.; Ghosh, A. K.; Mitsuya, H. GRL-0920, an Indole Chloropyridinyl Ester, Completely Blocks SARS-CoV-2 Infection. *mBio* **2020**, DOI: 10.1128/mBio.01833-20.
(117) Ghosh, A. K.; Takayama, J.; Aubin, Y.; Ratia, K.; Chaudhuri, R.; Baez, Y.; Sleeman, K.; Coughlin, M.; Nichols, D. B.; Mulhearn, D. C.; Prabhakar, B. S.; Baker, S. C.; Johnson, M. E.; Mesecar, A. D. Structure-based design, synthesis, and biological evaluation of a series of novel and reversible inhibitors for the severe acute respiratory syndrome-coronavirus papain-like protease. *J. Med. Chem.* **2009**, *52* (16), 5228−40.
(118) Lee, H.; Cao, S.; Hevener, K. E.; Truong, L.; Gatuz, J. L.; Patel, K.; Ghosh, A. K.; Johnson, M. E. Synergistic inhibitor binding to the papain-like protease of human SARS coronavirus: mechanistic and inhibitor design implications. *ChemMedChem.* **2013**, *8* (8), 1361−72.
(119) Lee, H.; Lei, H.; Santarsiero, B. D.; Gatuz, J. L.; Cao, S.; Rice, A. J.; Patel, K.; Szypulinski, M. Z.; Ojeda, I.; Ghosh, A. K.; Johnson, M. E. Inhibitor recognition specificity of MERS-CoV papain-like protease may differ from that of SARS-CoV. *ACS Chem. Biol.* **2015**, *10* (6), 1456−65.
(120) Mukae, H.; Yotsuyanagi, H.; Ohmagari, N.; Doi, Y.; Sakaguchi, H.; Sonoyama, T.; Ichihashi, G.; Sanaki, T.; Baba, K.; Tsuge, Y.; Uehara, T. Efficacy and Safety of Ensitrelvir in Patients With Mild-to-Moderate Coronavirus Disease 2019: The Phase 2b Part of a Randomized, Placebo-Controlled, Phase 2/3 Study. *Clinical Infectious Diseases* **2023**, *76* (8), 1403−1411.
(121) Boby, M. L.; Fearon, D.; Ferla, M.; Filep, M.; Koekemoer, L.; Robinson, M. C.; Chodera, J. D.; Lee, A. A.; London, N.; von Delft, A.; von Delft, F.; Achdout, H.; Aimon, A.; Alonzi, D. S.; Arbon, R.; Aschenbrenner, J. C.; Balcomb, B. H.; Bar-David, E.; Barr, H.; Ben-Shmuel, A.; Bennett, J.; Bilenko, V. A.; Borden, B.; Boulet, P.; Bowman, G. R.; Brewitz, L.; Brun, J.; Bvnbs, S.; Calmiano, M.; Carbery, A.; Carney, D. W.; Cattermole, E.; Chang, E.; Chernyshenko, E.; Clyde, A.; Coffland, J. E.; Cohen, G.; Cole, J. C.; Contini, A.; Cox, L.; Croll, T. I.; Cvitkovic, M.; De Jonghe, S.; Dias, A.; Donckers, K.; Dotson, D. L.; Douangamath, A.; Duberstein, S.; Dudgeon, T.; Dunnett, L. E.; Eastman, P.; Erez, N.; Eyermann, C. J.; Fairhead, M.; Fate, G.; Fedorov, O.; Fernandes, R. S.; Ferrins, L.;

https://doi.org/10.1021/acsomega.4c03023
ACS Omega 2024, 9, 34196−34219

Foster, R.; Foster, H.; Fraisse, L.; Gabizon, R.; García-Sastre, A.; Gawriljuk, V. O.; Gehrtz, P.; Gileadi, C.; Giroud, C.; Glass, W. G.; Glen, R. C.; Glinert, I.; Godoy, A. S.; Gorichko, M.; Gorrie-Stone, T.; Griffen, E. J.; Haneef, A.; Hassell Hart, S.; Heer, J.; Henry, M.; Hill, M.; Horrell, S.; Huang, Q. Y. J.; Huliak, V. D.; Hurley, M. F. D.; Israely, T.; Jajack, A.; Jansen, J.; Jnoff, E.; Jochmans, D.; John, T.; Kaminow, B.; Kang, L.; Kantsadi, A. L.; Kenny, P. W.; Kiappes, J. L.; Kinakh, S. O.; Kovar, B.; Krojer, T.; La, V. N. T.; Laghnimi-Hahn, S.; Lefker, B. A.; Levy, H.; Lithgo, R. M.; Logvinenko, I. G.; Lukacik, P.; Macdonald, H. B.; MacLean, E. M.; Makower, L. L.; Malla, T. R.; Marples, P. G.; Matviiuk, T.; McCorkindale, W.; McGovern, B. L.; Melamed, S.; Melnykov, K. P.; Michurin, O.; Miesen, P.; Mikolajek, H.; Milne, B. F.; Minh, D.; Morris, A.; Morris, G. M.; Morwitzer, M. J.; Moustakas, D.; Mowbray, C. E.; Nakamura, A. M.; Neto, J. B.; Neyts, J.; Nguyen, L.; Noske, G. D.; Oleinikovas, V.; Oliva, G.; Overheul, G. J.; Owen, C. D.; Pai, R.; Pan, J.; Paran, N.; Payne, A. M.; Perry, B.; Pingle, M.; Pinjari, J.; Politi, B.; Powell, A.; Pšenák, V.; Pulido, I.; Puni, R.; Rangel, V. L.; Reddi, R. N.; Rees, P.; Reid, S. P.; Reid, L.; Resnick, E.; Ripka, E. G.; Robinson, R. P.; Rodriguez-Guerra, J.; Rosales, R.; Rufa, D. A.; Saar, K.; Saikatendu, K. S.; Salah, E.; Schaller, D.; Scheen, J.; Schiffer, C. A.; Schofield, C. J.; Shafeev, M.; Shaikh, A.; Shaqra, A. M.; Shi, J.; Shurrush, K.; Singh, S.; Sittner, A.; Sjö, P.; Skyner, R.; Smalley, A.; Smeets, B.; Smilova, M. D.; Solmesky, L. J.; Spencer, J.; Strain-Damerell, C.; Swamy, V.; Tamir, H.; Taylor, J. C.; Tennant, R. E.; Thompson, W.; Thompson, A.; Tomásio, S.; Tomlinson, C. W. E.; Tsurupa, I. S.; Tumber, A.; Vakonakis, I.; van Rij, R. P.; Vangeel, L.; Varghese, F. S.; Vaschetto, M.; Vitner, E. B.; Voelz, V.; Volkamer, A.; Walsh, M. A.; Ward, W.; Weatherall, C.; Weiss, S.; White, K. M.; Wild, C. F.; Witt, K. D.; Wittmann, M.; Wright, N.; Yahalom-Ronen, Y.; Yilmaz, N. K.; Zaidmann, D.; Zhang, I.; Zidane, H.; Zitzmann, N.; Zvornicanin, S. N. Open science discovery of potent noncovalent SARS-CoV-2 main protease inhibitors. *Science* **2023**, *382* (6671), eabo7201.

(122) Yu, W.; Zhao, Y.; Ye, H.; Wu, N.; Liao, Y.; Chen, N.; Li, Z.; Wan, N.; Hao, H.; Yan, H.; Xiao, Y.; Lai, M. Structure-Based Design of a Dual-Targeted Covalent Inhibitor Against Papain-like and Main Proteases of SARS-CoV-2. *J. Med. Chem.* **2022**, *65* (24), 16252−16267.

(123) Jacobs, J.; Grum-Tokars, V.; Zhou, Y.; Turlington, M.; Saldanha, S. A.; Chase, P.; Eggler, A.; Dawson, E. S.; Baez-Santos, Y. M.; Tomar, S.; Mielech, A. M.; Baker, S. C.; Lindsley, C. W.; Hodder, P.; Mesecar, A.; Stauffer, S. R. Discovery, synthesis, and structure-based optimization of a series of N-(tert-butyl)-2-(N-arylamido)-2-(pyridin-3-yl) acetamides (ML188) as potent noncovalent small molecule inhibitors of the severe acute respiratory syndrome coronavirus (SARS-CoV) 3CL protease. *Journal of medicinal chemistry* **2013**, *56* (2), 534−46.

(124) Lockbaum, G. J.; Reyes, A. C.; Lee, J. M.; Tilvawala, R.; Nalivaika, E. A.; Ali, A.; Kurt Yilmaz, N.; Thompson, P. R.; Schiffer, C. A. Crystal Structure of SARS-CoV-2 Main Protease in Complex with the Non-Covalent Inhibitor ML188. *Viruses* **2021**, *13* (2), 174.

(125) Kitamura, N.; Sacco, M. D.; Ma, C.; Hu, Y.; Townsend, J. A.; Meng, X.; Zhang, F.; Zhang, X.; Ba, M.; Szeto, T.; Kukuljac, A.; Marty, M. T.; Schultz, D.; Cherry, S.; Xiang, Y.; Chen, Y.; Wang, J. Expedited Approach toward the Rational Design of Noncovalent SARS-CoV-2 Main Protease Inhibitors. *J. Med. Chem.* **2022**, *65* (4), 2848−2865.

(126) Andrianov, A. M.; Kornoushenko, Y. V.; Karpenko, A. D.; Bosko, I. P.; Tuzikov, A. V. Computational discovery of small drug-like compounds as potential inhibitors of SARS-CoV-2 main protease. *J. Biomol. Struct. Dyn.* **2021**, *39* (15), 5779−5791.

(127) Clyde, A.; Galanie, S.; Kneller, D. W.; Ma, H.; Babuji, Y.; Blaiszik, B.; Brace, A.; Brettin, T.; Chard, K.; Chard, R.; Coates, L.; Foster, I.; Hauner, D.; Kertesz, V.; Kumar, N.; Lee, H.; Li, Z.; Merzky, A.; Schmidt, J. G.; Tan, L.; Titov, M.; Trifan, A.; Turilli, M.; Van Dam, H.; Chennubhotla, S. C.; Jha, S.; Kovalevsky, A.; Ramanathan, A.; Head, M. S.; Stevens, R. High-Throughput Virtual Screening and Validation of a SARS-CoV-2 Main Protease Noncovalent Inhibitor. *J. Chem. Inf Model* **2022**, *62* (1), 116−128.

(128) Gao, S.; Sylvester, K.; Song, L.; Claff, T.; Jing, L.; Woodson, M.; Weiße, R. H.; Cheng, Y.; Schäkel, L.; Petry, M.; Gütschow, M.; Schiedel, A. C.; Sträter, N.; Kang, D.; Xu, S.; Toth, K.; Tavis, J.; Tollefson, A. E.; Müller, C. E.; Liu, X.; Zhan, P. Discovery and Crystallographic Studies of Trisubstituted Piperazine Derivatives as Non-Covalent SARS-CoV-2 Main Protease Inhibitors with High Target Specificity and Low Toxicity. *J. Med. Chem.* **2022**, *65* (19), 13343−13364.

(129) Zhang, J. W.; Xiong, Y.; Wang, F.; Zhang, F. M.; Yang, X.; Lin, G. Q.; Tian, P.; Ge, G.; Gao, D. Discovery of 9,10-dihydrophenanthrene derivatives as SARS-CoV-2 3CL(pro) inhibitors for treating COVID-19. *European journal of medicinal chemistry* **2022**, *228*, 114030.

(130) Zhang, K.; Wang, T.; Li, M.; Liu, M.; Tang, H.; Wang, L.; Ye, K.; Yang, J.; Jiang, S.; Xiao, Y.; Xie, Y.; Lu, M.; Zhang, X. Discovery of quinazolin-4-one-based non-covalent inhibitors targeting the severe acute respiratory syndrome coronavirus 2 main protease (SARS-CoV-2 M(pro)). *Eur. J. Med. Chem.* **2023**, *257*, 115487.

(131) Pérez-Vargas, J.; Worrall, L. J.; Olmstead, A. D.; Ton, A. T.; Lee, J.; Villanueva, I.; Thompson, C. A. H.; Dudek, S.; Ennis, S.; Smith, J. R.; Shapira, T.; De Guzman, J.; Gang, S.; Ban, F.; Vuckovic, M.; Bielecki, M.; Kovacic, S.; Kenward, C.; Hong, C. Y.; Gordon, D. G.; Levett, P. N.; Krajden, M.; Leduc, R.; Boudreault, P. L.; Niikura, M.; Paetzel, M.; Young, R. N.; Cherkasov, A.; Strynadka, N. C. J.; Jean, F. A novel class of broad-spectrum active-site-directed 3C-like protease inhibitors with nanomolar antiviral activity against highly immune-evasive SARS-CoV-2 Omicron subvariants. *Emerg Microbes Infect* **2023**, *12* (2), 2246594.

(132) Luttens, A.; Gullberg, H.; Abdurakhmanov, E.; Vo, D. D.; Akaberi, D.; Talibov, V. O.; Nekhotiaeva, N.; Vangeel, L.; De Jonghe, S.; Jochmans, D.; Krambrich, J.; Tas, A.; Lundgren, B.; Gravenfors, Y.; Craig, A. J.; Atilaw, Y.; Sandström, A.; Moodie, L. W. K.; Lundkvist, Å.; van Hemert, M. J.; Neyts, J.; Lennerstrand, J.; Kihlberg, J.; Sandberg, K.; Danielson, U. H.; Carlsson, J. Ultralarge Virtual Screening Identifies SARS-CoV-2 Main Protease Inhibitors with Broad-Spectrum Activity against Coronaviruses. *J. Am. Chem. Soc.* **2022**, *144* (7), 2905−2920.

(133) Pang, X.; Xu, W.; Liu, Y.; Li, H.; Chen, L. The research progress of SARS-CoV-2 main protease inhibitors from 2020 to 2022. *Eur. J. Med. Chem.* **2023**, *257*, 115491.

(134) Song, L.; Gao, S.; Ye, B.; Yang, M.; Cheng, Y.; Kang, D.; Yi, F.; Sun, J. P.; Menéndez-Arias, L.; Neyts, J.; Liu, X.; Zhan, P. Not Available. *Acta Pharm. Sin B* **2024**, *14* (1), 87−109.

(135) In *Herbal Medicine: Biomolecular and Clinical Aspects*, Benzie, I. F. F., Wachtel-Galor, S., Eds.; Taylor and Francis Group, LLC.: Boca Raton (FL), 2011.

(136) Mohamed, F. F.; Anhlan, D.; Schöfbänker, M.; Schreiber, A.; Classen, N.; Hensel, A.; Hempel, G.; Scholz, W.; Kühn, J.; Hrincius, E. R.; Ludwig, S. Hypericum perforatum and Its Ingredients Hypericin and Pseudohypericin Demonstrate an Antiviral Activity against SARS-CoV-2. *Pharmaceuticals (Basel, Switzerland)* **2022**, *15* (5), 530.

(137) Cammann, J.; Denzel, K.; Schilling, G.; Gross, G. G. Biosynthesis of gallotannins: beta-glucogallin-dependent formation of 1,2,3,4,6-pentagalloylglucose by enzymatic galloylation of 1,2,3,6-tetragalloylglucose. *Arch. Biochem. Biophys.* **1989**, *273* (1), 58−63.

(138) Zhang, J.; Li, L.; Kim, S. H.; Hagerman, A. E.; Lü, J. Anti-cancer, anti-diabetic and other pharmacologic and biological activities of penta-galloyl-glucose. *Pharm. Res.* **2009**, *26* (9), 2066−80.

(139) Botten, D.; Fugallo, G.; Fraternali, F.; Molteni, C. Structural Properties of Green Tea Catechins. *J. Phys. Chem. B* **2015**, *119* (40), 12860−7.

(140) Granja, A.; Frias, I.; Neves, A. R.; Pinheiro, M.; Reis, S. Therapeutic Potential of Epigallocatechin Gallate Nanodelivery Systems. *Biomed Res. Int.* **2017**, *2017*, 1.

(141) Chiou, W. C.; Chen, J. C.; Chen, Y. T.; Yang, J. M.; Hwang, L. H.; Lyu, Y. S.; Yang, H. Y.; Huang, C. The inhibitory effects of PGG and EGCG against the SARS-CoV-2 3C-like protease. *Biochem. Biophys. Res. Commun.* **2022**, *591*, 130−136.

https://doi.org/10.1021/acsomega.4c03023
ACS Omega 2024, 9, 34196−34219

(142) Dar, N. J.; Hamid, A.; Ahmad, M. Pharmacologic overview of Withania somnifera, the Indian Ginseng. *Cellular and molecular life sciences: CMLS* **2015**, *72* (23), 4445−60.
(143) Chakraborty, S.; Mallick, D.; Goswami, M.; Guengerich, F. P.; Chakrabarty, A.; Chowdhury, G. The Natural Products Withaferin A and Withanone from the Medicinal Herb Withania somnifera Are Covalent Inhibitors of the SARS-CoV-2 Main Protease. *J. Nat. Prod.* **2022**, *85* (10), 2340−2350.
(144) Shen, L.; Niu, J.; Wang, C.; Huang, B.; Wang, W.; Zhu, N.; Deng, Y.; Wang, H.; Ye, F.; Cen, S.; Tan, W. High-Throughput Screening and Identification of Potent Broad-Spectrum Inhibitors of Coronaviruses. *Journal of Virology* **2019**, DOI: 10.1128/JVI.00023-19.
(145) Choy, K. T.; Wong, A. Y.; Kaewpreedee, P.; Sia, S. F.; Chen, D.; Hui, K. P. Y.; Chu, D. K. W.; Chan, M. C. W.; Cheung, P. P.; Huang, X.; Peiris, M.; Yen, H. L. Remdesivir, lopinavir, emetine, and homoharringtonine inhibit SARS-CoV-2 replication in vitro. *Antiviral research* **2020**, *178*, 104786.
(146) Valipour, M. Different Aspects of Emetine's Capabilities as a Highly Potent SARS-CoV-2 Inhibitor against COVID-19. *ACS pharmacology & translational science* **2022**, *5* (6), 387−399.
(147) Liang, S.; Deng, X.; Lei, L.; Zheng, Y.; Ai, J.; Chen, L.; Xiong, H.; Mei, Z.; Cheng, Y. C.; Ren, Y. The Comparative Study of the Therapeutic Effects and Mechanism of Baicalin, Baicalein, and Their Combination on Ulcerative Colitis Rat. *Frontiers in pharmacology* **2019**, *10*, 1466.
(148) Dinda, B.; Dinda, S.; DasSharma, S.; Banik, R.; Chakraborty, A.; Dinda, M. Therapeutic potentials of baicalin and its aglycone, baicalein against inflammatory disorders. *European journal of medicinal chemistry* **2017**, *131*, 68−80.
(149) Fang, P.; Yu, M.; Shi, M.; Bo, P.; Gu, X.; Zhang, Z. Baicalin and its aglycone: a novel approach for treatment of metabolic disorders. *Pharmacological reports: PR* **2020**, *72* (1), 13−23.
(150) Su, H. X.; Yao, S.; Zhao, W. F.; Li, M. J.; Liu, J.; Shang, W. J.; Xie, H.; Ke, C. Q.; Hu, H. C.; Gao, M. N.; Yu, K. Q.; Liu, H.; Shen, J. S.; Tang, W.; Zhang, L. K.; Xiao, G. F.; Ni, L.; Wang, D. W.; Zuo, J. P.; Jiang, H. L.; Bai, F.; Wu, Y.; Ye, Y.; Xu, Y. C. Anti-SARS-CoV-2 activities in vitro of Shuanghuanglian preparations and bioactive ingredients. *Acta pharmacologica Sinica* **2020**, *41* (9), 1167−1177.
(151) Dinda, B.; Dinda, M.; Dinda, S.; De, U. C. An overview of anti-SARS-CoV-2 and anti-inflammatory potential of baicalein and its metabolite baicalin: Insights into molecular mechanisms. *Eur. J. Med. Chem.* **2023**, *258*, 115629.
(152) Cui, J.; Jia, J. Discovery of juglone and its derivatives as potent SARS-CoV-2 main proteinase inhibitors. *European journal of medicinal chemistry* **2021**, *225*, 113789.
(153) Chiou, W. C.; Huang, G. J.; Chang, T. Y.; Hsia, T. L.; Yu, H. Y.; Lo, J. M.; Fu, P. K.; Huang, C. Ovatodiolide inhibits SARS-CoV-2 replication and ameliorates pulmonary fibrosis through suppression of the TGF-β/TβRs signaling pathway. *Biomed Pharmacother* **2023**, *161*, 114481.
(154) Wasilewicz, A.; Kirchweger, B.; Bojkova, D.; Abi Saad, M. J.; Langeder, J.; Bütikofer, M.; Adelsberger, S.; Grienke, U.; Cinatl, J., Jr.; Petermann, O.; Scapozza, L.; Orts, J.; Kirchmair, J.; Rabenau, H. F.; Rollinger, J. M. Identification of Natural Products Inhibiting SARS-CoV-2 by Targeting Viral Proteases: A Combined in Silico and in Vitro Approach. *J. Nat. Prod* **2023**, *86* (2), 264−275.
(155) Langeder, J.; Döring, K.; Schmietendorf, H.; Grienke, U.; Schmidtke, M.; Rollinger, J. M. (1)H NMR-Based Biochemometric Analysis of Morus alba Extracts toward a Multipotent Herbal Anti-Infective. *J. Nat. Prod* **2023**, *86* (1), 8−17.
(156) Grienke, U.; Richter, M.; Walther, E.; Hoffmann, A.; Kirchmair, J.; Makarov, V.; Nietzsche, S.; Schmidtke, M.; Rollinger, J. M. Discovery of prenylated flavonoids with dual activity against influenza virus and Streptococcus pneumoniae. *Sci. Rep* **2016**, *6*, 27156.
(157) Park, Y. I.; Kim, J. H.; Lee, S.; Lee, I. S.; Park, J. Eupatin, a Flavonoid, Inhibits Coronavirus 3CL Protease and Replication. *Int. J. Mol. Sci.* **2023**, *24* (11), 9211.
(158) Pillai, U. J.; Cherian, L.; Taunk, K.; Iype, E.; Dutta, M. Identification of antiviral phytochemicals from cranberry as potential inhibitors of SARS-CoV-2 main protease (Mpro). *Int. J. Biol. Macromol.* **2024**, *261*, 129655.
(159) Jin, X.; Zhang, M.; Fu, B.; Li, M.; Yang, J.; Zhang, Z.; Li, C.; Zhang, H.; Wu, H.; Xue, W.; Liu, Y. Structure-Based Discovery of the SARS-CoV-2 Main Protease Noncovalent Inhibitors from Traditional Chinese Medicine. *J. Chem. Inf Model* **2024**, *64* (4), 1319−1330.

https://doi.org/10.1021/acsomega.4c03023
ACS Omega 2024, 9, 34196−34219